中 國 醫 藥 大 學
基礎醫學研究所
碩士學位論文

HMJ-53A 加速 Kv 通道慢性鈍化之機轉

Mechanisms for the acceleration of Kv channel slow inactivation by HMJ-53A

指 導 教 授 ：梁育民　副教授

研 究 生：趙家佳

中 華 民 國 九 十 七 年 六 月

誌謝辭

回想兩年前，剛剛進入研究所的我，對於研究有著很大的抱負，但卻不知道如何做起時，很幸運的進入到充滿歡樂氣氛的梁育民老師實驗室，並成為老師在台灣任教的第一位研究生。

兩年前，對電生理一知半解的我，一開始很惶恐但又很期待，又擔心自己做不好時，而我的指導教授-梁育民老師，很有耐心及細心的指導我，是一位很肯花時間在學生身上的好老師，使我在研究所中接受到一個完整的訓練過程。並從他的身上感受到研究及教學的熱誠，而讓我覺得做學問及研究是如此的有趣，對於思考問題更加縝密及有邏輯性，並影響我對於整個人生價值觀有著不同的想法，也因此讓我有繼續深造的動力；而對這位亦師亦友的梁老師之感謝，是無法用三言兩語形容-但真得很謝謝您，這段時間的用心栽培及指導。

感謝我的口試委員鄭瑞棠老師及鄭志鴻老師在口試過程中的專業指導，及建議我往後實驗方向，並引導我對於研究思考範圍更加廣闊，讓我受益良多。

也要謝謝這兩年來醫研所及生理科所有老師的指導，讓我對於口頭報告、思考問題及研究問題的批判，有很大的進步。另外，還要謝謝惠華姐在生理實驗課上的各項幫忙，也要謝謝醫研所麗如姐，協助處理我們研究生各項業務。

在實驗室一開始起步時，因林靜茹及許明志老師實驗室的全體成員幫忙，才讓我們能順利運作，謝謝你們。也要謝謝醫研所二年級的全體同學，大家的互相扶持及幫忙，才能開心及順利完成這兩年學業。並要感謝實驗室所有成員，因大家相處融洽及互相幫忙，才讓整個實驗室的運作順利。

再來我要謝謝我的家人及未來的家人，特別是我的母親，在背後一直默默的支持我，不讓我有任何顧慮的專心研究，要不是你們的支持，我也不可能順利畢業，謝謝你們!

這段研究生生涯，過程中雖有苦有笑有甜，但現在回想起來，全都是美妙的回憶也嘗到甜美的果實，不會忘記這裡的點點滴滴，我將會帶著這些果實，繼續充實我自己，並往上邁進。最後，再次感謝這一路所有幫助過也曾關心過我的人，謝謝你們。

研究生　趙家佳　謹識

民國九十七年六月二十三日 於台中

總目錄

頁次

圖表目錄

頁次

中文摘要

在可興奮性細胞，例如，神經細胞和內分泌細胞，利用電壓調控鉀離子(Kv)通道，使其膜電位於去極化後可復極化。某些Kv通道在去極化之過程中，會表現慢性鈍化之現象，此鈍化作用會使Kv通道產生某種形式的關閉，而其發生是因通道裡離子選擇性過濾器壓縮。至今，尚未有一個針對此慢性鈍化之特異性的探測藥物。我們發現一個新的藥物，HMJ-53A (30 μM)在小鼠神經瘤細胞株(N2A)上，有選擇性的加速Kv通道之慢性鈍化（沒加與有加HMJ-53A之衰退 τ，分別為1677 ± 120 ms 和 85.6 ± 7.7 ms）。HMJ-53A把Kv通道穩定鈍化曲線左移12mV，且不影響其活化階段。此外，我們在微細玻璃管電極內（細胞內）加入HMJ-53A，並不會產生加速Kv通道之慢性鈍化現象；而從此數據顯示，HMJ-53A作用在細胞外而非細胞內。HMJ-53A阻斷Kv通道上鉀離子外流，而所測得之電流，不需要Kv通道開啟。此外，HMJ-53A之阻斷Kv通道電流及鈍化之時間常數，不會受到去極化程度及細胞內鉀離子濃度的影響。所以，HMJ-53A不會直接堵塞Kv通道之孔洞，而是讓圍著通道孔之選擇性過濾器加快壓縮。綜合以上的結果可以得知，HMJ-53A可有選擇性的加速Kv通道之慢性鈍化，可作為探測Kv通道鈍化閥門之對抗藥。

Abstract

Voltage-gated K^+ (Kv) channels are important in repolarization of excitable cells such as neurons and endocrine cells. Kv channel gating exhibits slow inactivation (slow current decay) during continuous depolarization. The molecular mechanism involved in such slow inactivation is not completely understood, but evidence has suggested that it involves a restriction of the outer channel pore surrounding the selectivity filter. Pharmacological tools probing this slow inactivation process are scarce. In this work we reported that bath application of HMJ-53A (30 μM), a novel compound, could drastically speed up the slow decay (decay τ = 1677±120 ms and 85.6 ±7.7 ms, respectively, in the absence and presence of HMJ-53A) of Kv currents in neuroblastoma N2A cells. HMJ-53A also significantly left-shifted the steady-state inactivation curve by 12 mV. HMJ-53A, however, did not affect voltage-dependence of activation and the kinetics of channel activation. Intracellular application of this drug through patch pipette dialysis was ineffective at all in accelerating the slow current decay, suggesting that HMJ-53A acted extracellularly. Blockade of currents by HMJ-53A did not require an open state of channels. In addition, the

inactivation time constants and percentage block of Kv currents in the presence of HMJ-53A were independent of the (i) degree of depolarization and (ii) intracellular K^+ concentration. Therefore, this drug did not appear to directly occlude the outer channel pore during stimulation (depolarization). Taken together, our results suggest that HMJ-53A selectively affected (accelerated) the slow inactivation gating process of Kv channels, and could thus be a selective and novel probe for the inactivation gate.

第一章：前言

在細胞膜上有許多的離子通道，扮演各種不同功能，而控制離子通道的開關因子包括：神經傳送素、荷爾蒙、膜電位、壓力、光及代謝產物等。可興奮性細胞受到刺激時，鈉與鉀離子通道隨即打開，例如：神經細胞因受到藥物及細胞膜電位改變等刺激；而上述因素導致，鈉離子通道開啟，鈉離子進入細胞膜內，造成膜電位去極化(depolarization) (Berne et al., 1998)。接著鈉離子通道開始關閉，鈉離子無法進入細胞內，此時，鉀離子通道開啟，鉀離子開始往細胞外移動，使細胞膜漸漸恢復其負電性，此稱為復極化(repolarization)，此時膜電位稍微超過靜止膜電位，而形成過極化(hyperpolarization)，進而漸漸達到鉀離子通道平衡電位，鉀離子通道關閉，回到靜止膜電位；這就是在興奮性細胞上的電性活動階段。

第一節：鉀離子通道的種類及特性

目前已知鉀離子通道的種類很多，最多被研究者包括下列幾種(Hille, 2001)：

1. 鈣離子活化鉀離子通道 [Ca^{2+}-activated K^+ (K_{Ca}) channels]：

當細胞膜電位發生改變,細胞內鈣離子濃度增加 1–10 μM，並使細胞呈現去極化現象，此時鉀離子通道開啟，鉀離子從細胞內流出；再依傳導性的大小，可分為 big K(Ca) 【BK】、intermediate K(Ca)【IK】及 small K(Ca)【SK】通道。而目前已知，此通道存在於神經、心臟及骨骼肌肉細胞…等中 (Poolos and Johnston, 1999; Wang et al., 2008)。

2. 漏鉀通道 [Leak K^+ channel]：

此通道結構是由 4 個穿膜片段 (S1-S4) 連接及 2 個 P-loop 所構成的。而其一直呈現開啟狀態，主要是受膜電位及細胞內外鉀離子濃度影響。當漏鉀離子通道開啟時，為了要抗衡化學梯度，而在此通道中，必須產生膜內相對於膜外較負的電位差，而膜內的負電荷會拉住鉀離子，使鉀離子無法往膜外流動，使鉀電流動達到平衡。所以，此通道的主要功能是維持靜止膜電位 (Goldstein et al., 1996)。而此通道會受到細胞外 pH 值變化及麻醉藥（例如：Bupivacaine）影響 (Bayliss et al., 2001; Kindler et al., 1999)。

3. 內流型鉀離子通道 [Inward rectifier K^+ (Kir) channels]：

調控主要是受膜電位的改變而開啟；當細胞膜電位低於平衡電位時，會使此通道開啟，並使鉀離子往細胞內流入；而

其特別的是，並不會因為隨著膜電位增加，而使鉀離子往細胞外流動 (Hille, 2001)；最主要調控此通道者，是靠著細胞內的陽離子：Mg^{2+}及 putrescine、spermidine、spermine，去阻止鉀離子往細胞外移動 (Loussouarn et al., 2002)。Kir 通道多存於心臟及神經細胞…等。

4. ATP 敏感性型鉀離子通道 [Adenosine 5′- triphosphate - sensitive K^+ (K_{ATP}) channels]：

結構是由Kir6.x（6.1或6.2）及sulfonylurea接受器（SUR1或SUR2）所構成。此通道的開啟與關閉是受細胞內ATP和ADP的濃度影響，也就是當細胞內[ATP]/[ADP]下降，會使此通道開啟，而現今在神經保護機制及內分泌的調控…等，占有很重要的角色。例如：當人體處於飽食狀態，胰島上的β-細胞內[ATP]/[ADP]比例上升，讓此通道關閉，鉀離子不往細胞外流動，使β-細胞去極化並興奮，再使Ca通道開啟，而使胰島素釋放，進而降低血糖。目前已知此通道存在於神經、心臟及胰島細胞…等中 (Leung et al., 2006; Sun et al., 2007)；而現今對於K_{ATP}通道對神經保護之作用已被證實但機制卻不清楚 (Jahangir and Terzic, 2005; Yamada and Inagaki, 2005)。

5. 電壓調控鉀離子通道 [Voltage - gated K^+ (Kv) channels]：

Kv 通道是鉀離子通道種類中，目前最多被廣泛研究的一種，而其在興奮性細胞之動作電位中，占有重要的角色。

而 Kv 通道在動作電位中之復極化，控制鉀離子往細胞外流動上扮演很重要的角色；尤其在興奮性細胞：內分泌、肌肉、神經及心肌細胞...等。而另一方面，Kv通道會受到閥門影響，去控制其開關；當 Kv 通道開啟的過程稱為活化 (activation)，在通道開啟後隨之漸漸失去通透鉀離子能力稱為鈍化 (inactivation)，而當復極化之後，Kv 通道會回到關閉的狀態，此過程稱為去活化 (deactivation)。這就是整個 Kv 通道從開啟到關閉的整個過程。

第二節：電壓調控鉀離子通道〔Voltage-gated K^+ (Kv) channels〕結構

Kv通道構造是由四個α-膜蛋白次單元 (α-subunits)（圖1）而環繞著中心孔所構成，而每個α-subunit是由六條穿膜片段 (S1-S6)連接而成（圖2），每個α-subunit包含C端 (C-terminus)和N端 (N-terminus)，皆位於細胞內側 (Choe et al., 1999)。

S4因帶有規則排列的七個正電鹼性胺基酸，可以感應電場的變化，而S4最靠近外側的四個鹼性胺基酸為主要的感應電荷位置，而在通

道關閉狀態時是位在近細胞膜內側內，當通道受電場變化而開啟時，四個鹼性胺基酸是位在近細胞膜外側上。S4運動方式主要有兩種：

第一種：S4利用旋轉並往細胞外位移的方式運動。

第二種：S4位於通道蛋白質的外圍與細胞膜接觸，利用擺動的方式移動。

2003年，Mackinnon團隊利用*Aeropyrum pernix*的嗜熱性古細菌(thermophilic archaebacterium) 分離出鉀離子通道蛋白KvAP，而其胺基酸序列與真核細胞的Kv通道蛋白非常相近，並以結晶X-ray繞射技術做出KvAP電壓關閉性的鉀離子通道結晶結構，其感應電荷(gating charges)位置在離子通道最外圍，是位在S3b-S4、helix-turn-helix結構中，當細胞去極化時，整個電壓感測器擺動至細胞外，進而牽動孔洞上S6使通道開啟，而此種模式稱之為paddle model (Jiang et al., 2003)。

鉀離子通道上S5和S6間的P-loop是由 -TXXTXGYGD- (-thr-X-X-thr-X-gly-tyr-gly-glu-)此特徵序列組成，而由膜外側伸入膜內後，做一個轉折再往膜外側伸出，形成一個圈環且是整個通道最狹窄的孔洞。Kv通道中，其中-TVGYG- (-thr-V-gly-tyr-gly-)構成離子選擇最關鍵的部位稱之為選擇性過濾器 (selectivity filter)（圖3）(Choe, 2002; Yellen, 2002)；因為選擇性過濾器相當狹窄，依凡得瓦

力定律 (van der Waal's law)，鉀離子在通過時必須脫去外側層水合分子 (hydration waters)，在選擇性過濾通道上羰基的氧原子(carbonyl oxygens)則取代鉀離子外側層水分子，與鉀離子結合。由於鉀離子的體積大小能精確的配合選擇性過濾通道大小與羰基的氧原子皆都可碰到，而能量得失取之平衡；雖鈉離子的體積較鉀離子小卻無法精確的配合此過濾通道大小，無法平衡，所以，這也就是鉀離子通道能選擇性的只供鉀離子通過之原因 (Choe et al., 1999; Doyle et al., 1998)。

Kv通道的整個結構：由S1-S6六個穿膜片段 (six transmembrane domain, 6TM)，構成一個次單位，其間S5與S6連接一條P-loop (P)組成，稱為6TM/P (Hille, 2001)。 Kv通道的功能：可將膜電位拉回至靜止膜電位，而使得動作電位在適當的時間內形成，且可結束一連串的放電，並在重複性的極化模式中、調控動作電位之輪廓與間隔時間 (Nerbonne, 2000)。

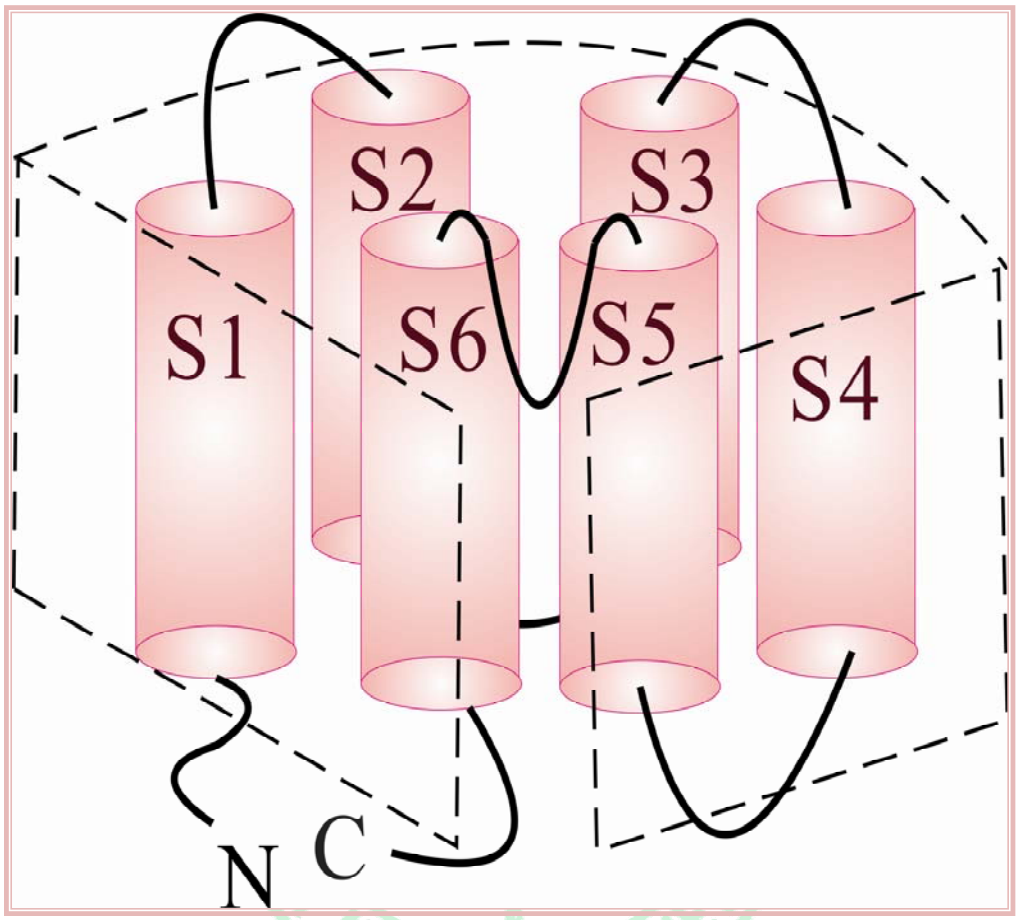

圖 1：Kv 通道上之單個 α-膜蛋白次單元 (α- subunit)立體結構：由六個(S1-S6)穿膜蛋白連接而成一個 α- subunit，而一個 Kv 通道由四個 α- subunit 所組成，其 N 端與 C 端皆位於細胞內側。modify (Choe et al., 1999)。

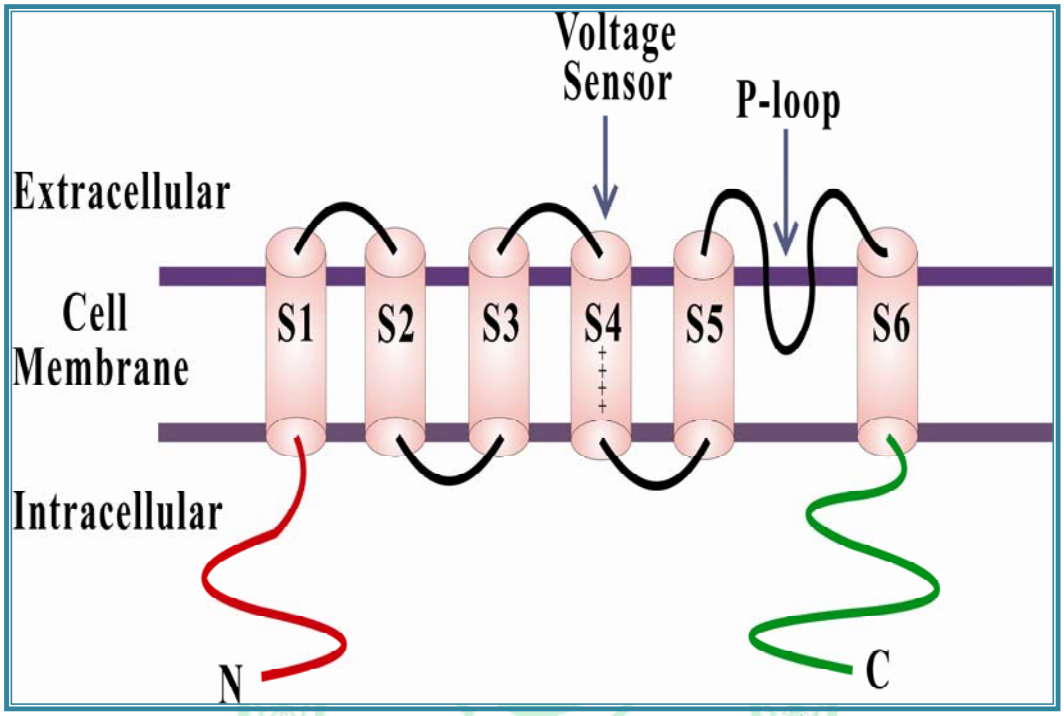

圖 2：Kv 通道上，每個 α- subunit 是由六條穿膜蛋白(S1-S6)連接而成，包含 C-terminus 和 N-terminus 皆位於細胞內側，S4 為電壓感應器。

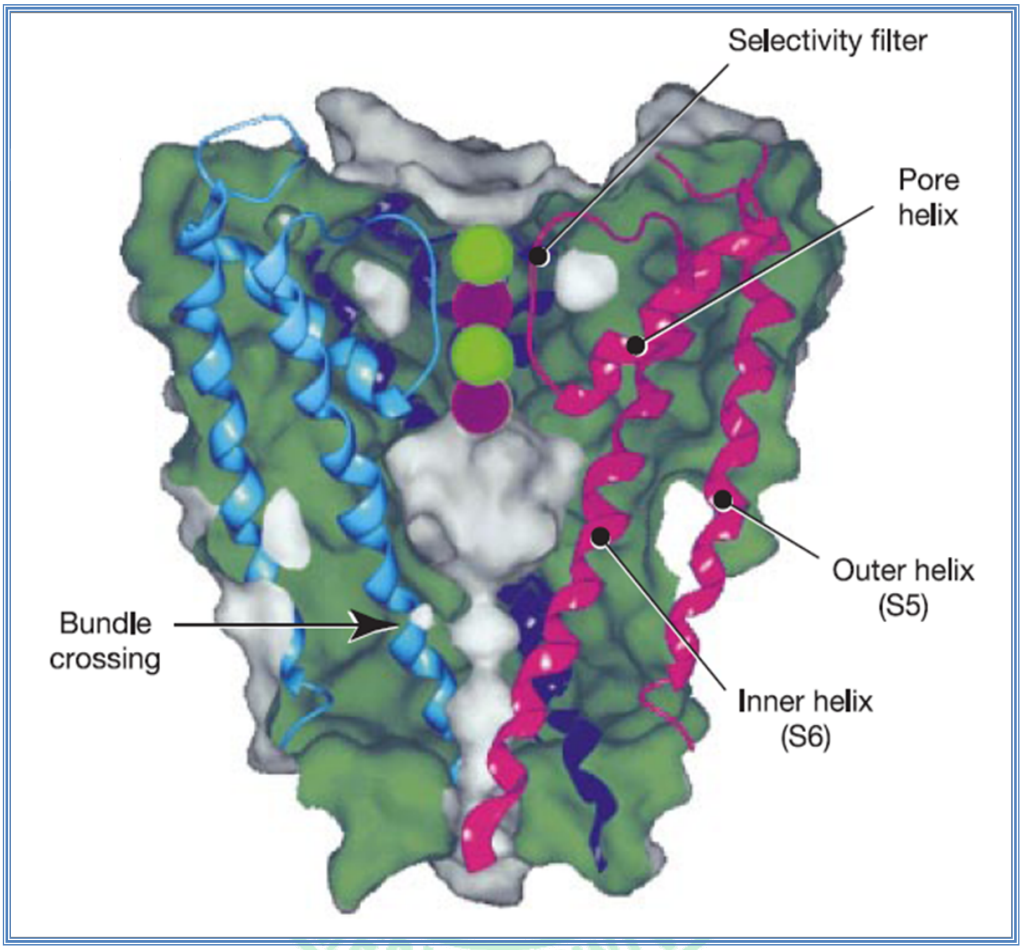

圖 3：Kv 通道之選擇性過濾器(selectivity filter)，鉀離子經過此過濾器時，須經過脫水的過程後，與過濾器中的氧原子結合後，往細胞膜外流出 (Choe, 2002)。

第三節：電壓調控鉀離子通道之鈍化 (inactivation)

當細胞膜去極化時，S4能感測電場變化而使S6移動，進而使得鉀離子通道活化閥門 (activation gate)開啟，而允許細胞內的鉀離子往細胞外流出 (Choe, 2002; Yellen, 2002)。而當活化閥門開啟後，鉀離子通道接著走向鈍化 (inactivation)階段，而此階段必須是通道開啟後產生。復極化後，通道走向去活化 (deactivation)階段，使通道關閉，而鈍化之通道亦慢慢回復 (recovery) (Hille, 2001)。

在電壓調控鉀離子通道上，鈍化主要分成快速及慢速兩大類：

第一類：N型鈍化（N - type inactivation），因發生鈍化速度快約為100至200ms，又稱為快速型鈍化（fast inactivation），見於Kv1.4、Kv3.1、Kv3.4和Kv4.2通道上 (Kukuljan et al., 1995)。

第二類：C型鈍化（C - type inactivation），大部分Kv通道上皆可見，因其鈍化速度長達一秒至幾秒鐘，速度很慢，又稱為慢速型鈍化（slow inactivation） (Kurata and Fedida, 2006)，可見於Kv1.5和 Kv2.1通道上 (Andalib et al., 2004; Kurata et al., 2001)。

第四節：電壓調控鉀離子通道中N型鈍化

在Kv通道中，N型鈍化發生在六個穿膜片段所組成的每個次單位上的N端，而此端是位於細胞內連接著20個胺基酸所組成的球 (ball)與21至80號胺基酸所形成的鏈 (chain)，稱之為“ball and chain”。當細胞膜因膜電位去極化的刺激，使Kv通道活化時，導致通道蛋白結構變化，閥門開啟，細胞膜內之通道孔洞內露出鈍化球接合的位置，此時Kv通道上N端的“ball and chain”由下往上堵住孔洞而形成快速鈍化，並防止鉀離子通過此孔洞 (Gulbis et al., 2000)，再當細胞膜復極化後，因電場改變而產生回復作用，並使球離開孔洞，再產生去活化，使通道回到休息的狀態（圖4）。

若快速給予過極化時，球無法及時在通道關閉前掉落，此時在通道內會產生“卡住” (trapped)之現象 (Holmgren et al., 1996)。若將鉀離子通道上的N端（20個胺基酸，ball）除掉，可去除N-型鈍化，另外，假若切除N端後，合成20個胺基酸序列於細胞內，發現可以回復N型鈍化反應，且發生速率與球之濃度成正比的現象 (Zagotta et al., 1990)。

所以，Kv通道內的四個鈍化球受電位改變移動後在細胞內卡上孔洞，形成N型鈍化，而這四個球皆有相同機率產生這樣的結果，只要其中一個球即可，速度很快的達成N型鈍化，所以，四個鈍化球是一個鈍化球達成N型鈍化的四倍速率 (MacKinnon et al., 1993)。

而TEA (tetraethylammonium chloride)已是現今普遍用來探討阻斷N型鈍化的鉀離子阻斷劑，其阻斷方式乃是經由細胞內往上堵住通道內孔，而使鉀離子通道上之N端之“ball and chain”無法堵住內孔，使N型鈍化無法達成 (Baukrowitz and Yellen, 1996; Choi et al., 1991; Choi et al., 1993)。

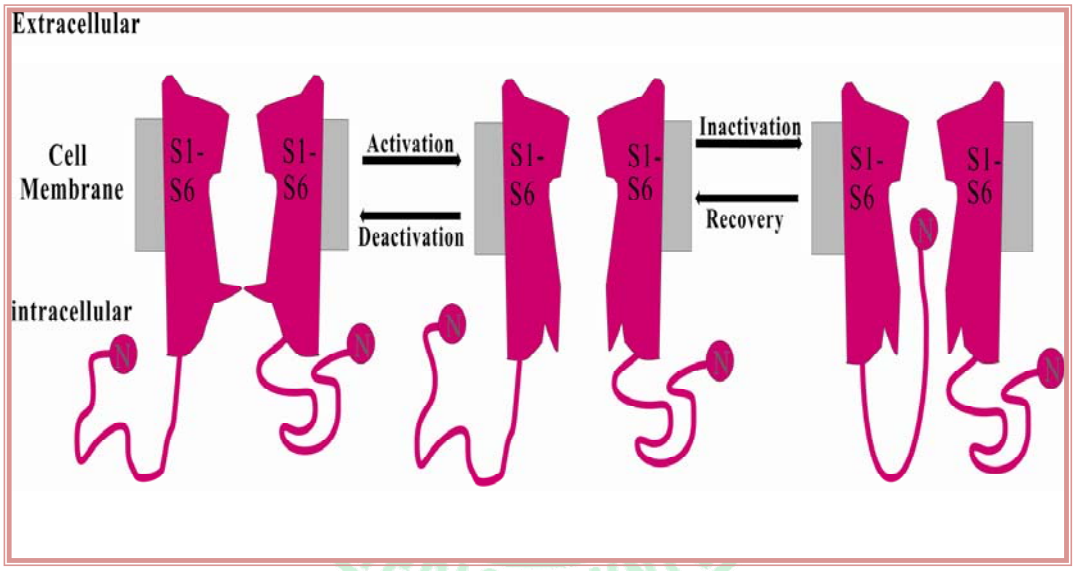

圖 4 ：N-type inactivation

鉀離子通道上之 N 型鈍化

第五節：電壓調控鉀離子通道中 C 型鈍化

慢性鈍化幾乎發生在所有的Kv通道上，不論有無N型鈍化，而此種慢性鈍化現象常常會持續幾秒鐘，且發生在通道持續不斷的去極化期間 (Kurata and Fedida, 2006)。慢性鈍化現象又稱為C型鈍化

（C-type inactivation）且發生在許多不同種類的Kv通道上，例如：Kv1.5和Kv2.1通道 (Andalib et al., 2004; Kurata et al., 2001)。

現今來說，這種複雜的C型鈍化機制，並不是完全清楚了解，但現今有研究顯示：C型鈍化現象是通道外孔的選擇性過濾器產生倒塌或壓縮而造成結構改變 (Kurata and Fedida, 2006)。而至今已知其作用機制：當細胞膜因膜電位去極化的刺激，使Kv通道活化時，導致通道蛋白結構變化，閥門開啟，進而使通道外孔的選擇性過濾器產生收縮及壓縮而造成結構不穩定，形成慢速鈍化，而細胞膜處於復極化狀態後，因後電場改變而產生回復作用，並使通道孔洞內的選擇性過濾器慢慢的往外回復，通道繼而再產生去活化，使通道回到休息的狀態，並準備好下一次的活化及放電（圖5）。

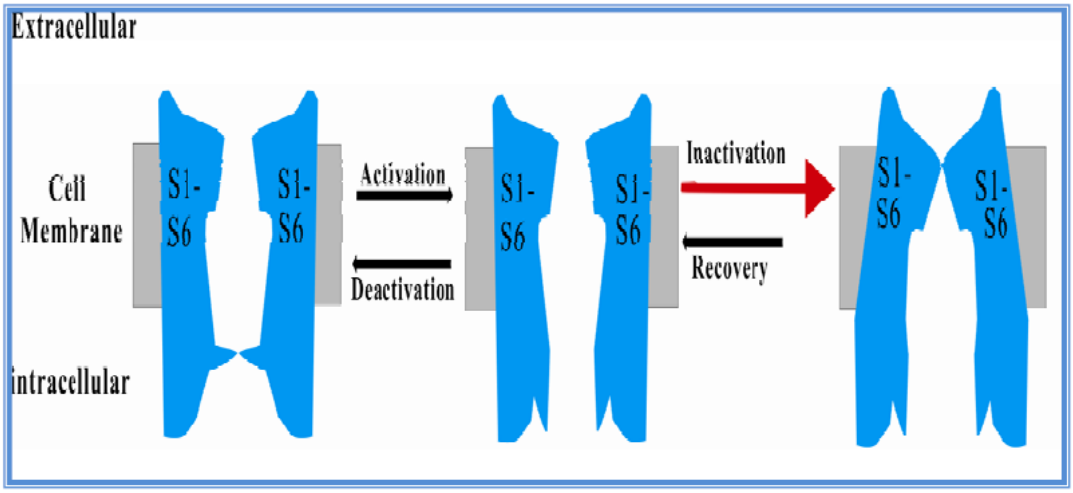

圖5：C-type inactivation

鉀離子通道上之 C 型鈍化

哪些胺基酸影響C型鈍化？最早是在*Shaker* 通道（Kv1家族）外孔上的threonine（T）位置449的改變可以加快（T449E,T449A, T449K）或減慢（T449Y, T449V）C型鈍化速度，也就是改變T449：arginine（R）、lysine（K）、alanine（A）或 glutamate（E）這些胺基酸，會加快其速度；另一方面，改變為valine（V）或tyrosine（Y）會減慢C型鈍化速度。若切斷N端只存有C端後，並不會停止其鈍化現象，而定義為C型鈍化 (Hoshi et al., 1990; Lopez-Barneo et al., 1993)。

1998年，學者發現，在Kv1.3及1.5通道上，細胞外加入低濃度(30-50 μM)鉀離子，而鉀離子與通道上的選擇性過濾器親和力增加，並大於鈉離子，而抑制C型鈍化 (Kiss et al., 1998)。*Shaker*通道上，增加細胞外鉀離子的濃度及加入TEA，皆會減慢C型鈍化的速度。另外在Kv1.3中，發現細胞內酪胺酸磷酸化 (tyrosine kinase phosphorylation)可造成C型鈍化速度很輕微的加快，但作者卻無法定義出磷酸化會影響C型鈍化的相關性或影響Kv1.3哪個胺基酸 (Bowlby et al., 1997)。

2007年有學者研究出：利用能夠穩定二級結構的氫鍵 (hydrogen bonds)去探討選擇性過濾器上的殘基與鄰近在通道外孔上的helix之間的相關性及重要性，而去證實C型鈍化機制 (Cordero-Morales et al., 2007)。因此在Kv1.2上, 把Val370改變成Glu370（圖6），在活

化Kv1.2後，選擇性過濾器上的Glu370可與Asp379作用更強之相互牽引，使過濾器不穩定（或倒塌），隨之產生C型鈍化。當回復時，Glu370與Asp379會互相彈開，隨之去活化後，通道回到休息狀態(Cordero-Morales et al., 2007)（圖7）。

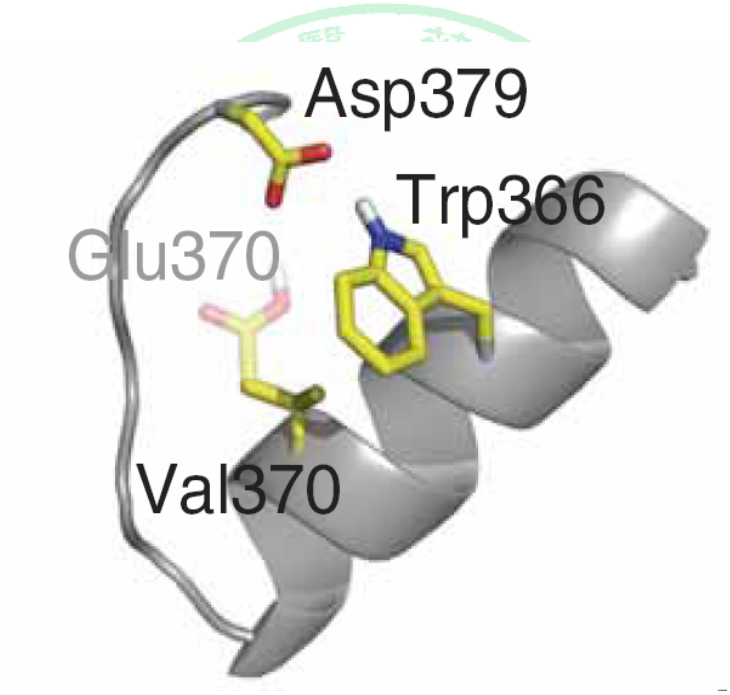

圖 6：在 Kv1.2 通道上，把原本 Val370 突變成 Glu370，發現 Glu370 與 Asp379 會更強地相互牽引，產生 C 型鈍化(Cordero-Morales et al., 2007)。

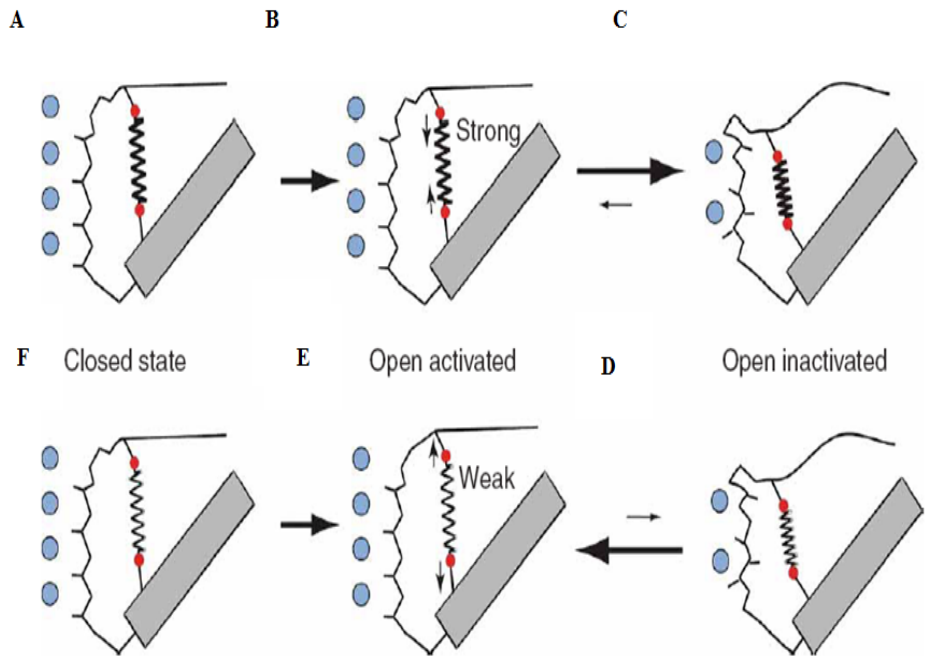

圖7：Kv1.2通道（A）通道處於休息狀態（B）選擇性過濾器上的Glu370與Asp379（兩個紅點表示）會相互牽引（C）隨之產生C型鈍化（D）此過程即是選擇性過濾器倒塌，而使鉀離子無法順利通過此通道（E）回復，Glu370與Asp379互相彈開（F）去活化後，通道回到休息狀態 (Cordero-Morales et al., 2007) 。

鉀離子通道的鈍化作用影響動作電位的輪廓及頻率，因此對於興奮細胞的調節是相當重要，例如：神經細胞 (Hille, 2001)。而藥物改變Kv通道的鈍化閥門也就是能改變神經細胞的興奮性，例如：4-acetamido-4'-isothiocyano-2,2'-disulphonic stilbene (SITS) 和 N-bromoacetamide (NBA)，已在腦垂下體細胞GH3中證實，能抑制Kv通道的N型鈍化 (Oxford and Wagoner, 1989)。

然而，目前尚無專一及選擇性的藥物去作為探測藥物進而探討Kv通道之C型鈍化。進而與侯曼貞老師合作新藥開發，篩選HMJ系列合成物過程中，發現此系列合成物中之HMJ-53A能影響Kv通道，而先前已發表其抗凝血作用藥效比Aspirin強，可以抑制花生四稀酸所造成的血小板凝集疾病 (IC_{50}：1.60 μM) (Hour et al., 2000)，這也讓我們懷疑所產生的抗凝血作用，是否因為阻斷離子通道所產生的呢？

所以，在此研究工作中，我們利用已知表達Kv通道的小鼠神經瘤N2A(mouse neuroblastoma)細胞，並著手探討HMJ-53A是如何影響Kv通道。結果發現此細胞上之Kv通道存有C型鈍化現象，且經由我們強而有力的結果顯示，HMJ-53A作用在細胞外而非細胞內，並大幅度的加速C型鈍化卻不影響Kv通道上的活化閥門。這些結果顯示HMJ-53A能當作一個新穎的合成物，去探測C型鈍化閥門。

第二章：研究方法

第一節：細胞培養

N2A (mouse neuroblastoma)為小鼠神經瘤細胞株，生長於37℃、5％CO_2培養箱，培養基為Dulbemlo's modified Eagle's medium (DMEM) (Gibco)、10% fetal bovine serum (FBS) (Invitrogen, Carlsbad, CA) 及 1 ％ penicillin-streptomycin (100 units/ml, 100 μg/ml) (Invitrogen)，為黏附型細胞，繼代培養方式：抽掉上清液，再用Dulbemlo's Phosphate Buffered Saline(PBS) (Sigma-Aldrich)沖兩次後，再加入1ml trypsin (0.25％, Invitrogen)，等待一分半鐘，再加入培養基6ml，然後放入離心管離心（900rpm、5分鐘）。之後，抽掉上清液，再加入1ml培養基，混合均勻，再加入少許的混合液至已有培養基的培養皿中，再放置培養箱中，三至四天後繼代。

PC-12 為大鼠腎上腺嗜鉻細胞瘤細胞株(Rat adrenal pheochromocytoma cells)，生長於37℃、5％CO_2培養箱，培養基為Dulbemlo's modified Eagle's medium (DMEM) (Gibco)、10% fetal bovine serum(FBS) (Invitrogen, Carlsbad, CA) 及 1 ％ penicillin-streptomycin (100 units/ml, 100 μg/ml) (Invitrogen)，為半懸浮型細胞，而其繼代培養方式：由原本培養皿中的培養基沖下細胞，再加入離心管離心（900rpm、3分鐘），抽掉上清液，再加入1ml培

養基，混合均勻，再加入少許的混合液至已有培養基的培養皿中，再放置培養箱中，約四至五天後繼代。

第二節：藥劑

1. HMJ-53A於中國醫藥大學藥學院藥學系侯曼貞老師實驗室取得。儲存藥物溶液濃度為100 mM，溶化於Dimethyl Sulfoxide(DMSO)。其結構式與合成程序如圖A。HMJ-53A對細胞沒有毒性，因加完HMJ-53A ，20分鐘後，利用trypan blue（10倍稀釋）測試N2A細胞存活率，而其存活率>95%。

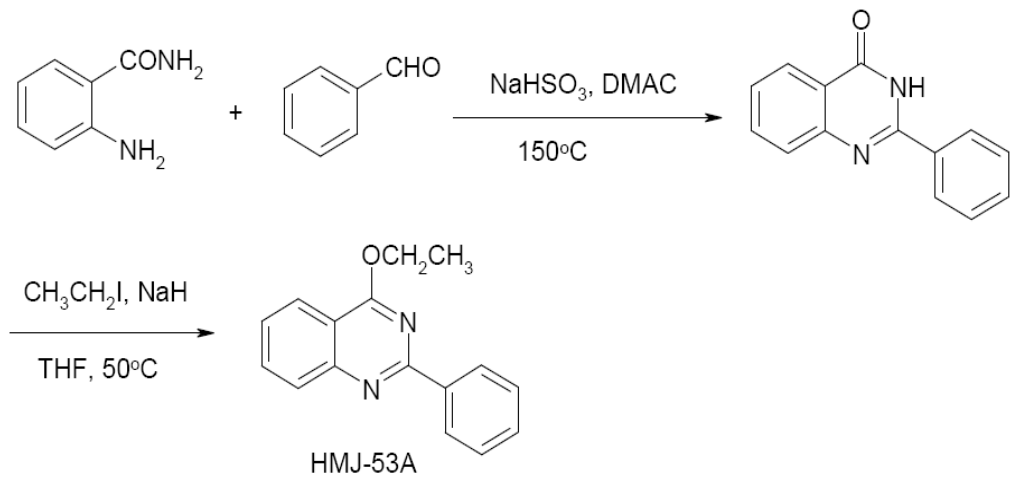

圖A：HMJ-53A結構式與合成程序

2. 其他HMJ系列之藥物（HMJ-1、HMJ-29A及HMJ-73A）皆從中國醫藥大學藥學院藥學系侯曼貞老師實驗室取得，儲存藥物溶液濃度為50-100 mM，溶化於DMSO，而它們的結構式如圖B。

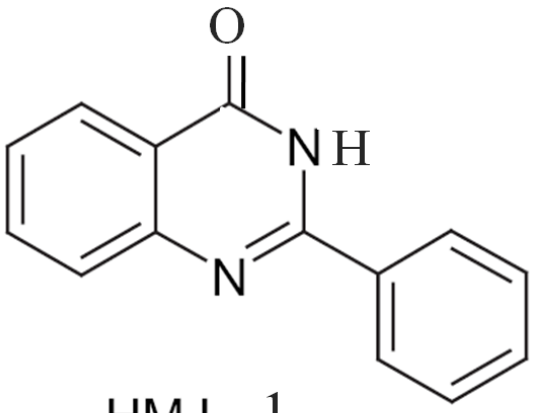

HMJ - 1

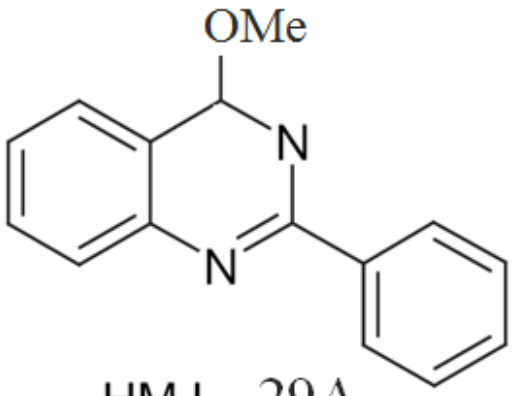

HMJ - 29A

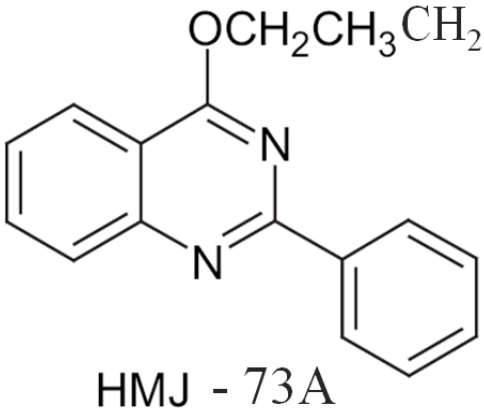

HMJ - 73A

圖 B：HMJ 系列之藥物結構式

3. TEA Cl（tetraethylammonium chloride）鉀離子通道阻斷劑，購買於Sigma-Aldrich (St. Louis, MO,USA)，儲存藥物溶液濃度為1 M，溶解於millipore water。

4. Staurosporine為非選擇性蛋白酶抑制劑，購買於Tocris (USA)，儲存藥物溶液濃度為100 μM，溶解於DMSO。

第三節：轉殖過程

pcDNA3-Kv2.1及pEGFP之cDNA，從加拿大多倫多大學的Professor Gaisano實驗室取得。再從裝有pcDNA3-Kv2.1及pEGFP之cDNA的微量離心管中，分別取出 3 μg及 1 μg加至無菌微量離心管中，並與Opti-MEM (Invitrogen, USA) (44 μl)混合均勻，等待20分鐘；而在等待過程中，把Lipofectamine™ 2000 (Invitrogen, USA)10 μl與40 μl的Opti-MEM，混合均勻並等待5分鐘。

之後，將兩個部分混合均勻，並再等待20分鐘，把有N2A細胞的3.5 cm 培養皿，用PBS沖洗三次，加入無抗生素的culture medium (DMEM內含有10%FBS) 2 ml；把上述已過了20分鐘之混合物，共100 μl加入至培養皿中，放至CO_2培養箱過一晚後，用螢光顯微鏡(Excitation：484nm，Emission：510nm)觀察細胞是否有轉殖成功；

假如成功會見到綠色的細胞；因為pEGFP (maker)已順利送至細胞核內，並已分別表達在細胞質及膜上，再經由顯微鏡上藍光激發，可見綠細胞，這就代表pcDNA3-Kv2.1也應該進入細胞了。如此，細胞可以繼代分盤，隔日即可做電生理記錄。

第四節：電生理（Electrophysiology）紀錄方法

一、溶液準備 (Leung et al., 2003)：

1. 細胞外液 Bath solution (mM)：140 NaCl , 4 KCl , 1 $MgCl_2$, 2 $CaCl_2$, 10 HEPES（用NaOH調整至pH 7.4）。
2. 細胞內液 Intracellular solution (mM)：140 KCl , 1 $MgCl_2$, 1 EGTA , 10 HEPES , 5 MgATP（用KOH調整至pH 7.25）。
3. 微細玻璃管電極 （thin-walled borosilicate glass tubes）（OD 1.5 mm , ID 1.10 mm , Sutter Instrument , Novato , CA），用 puller （P-87 , Sutter Instrument）加熱拉開成兩根，再用 microforge （Narishige Instruments,Inc., Sarasota, FL）加熱打磨。

二、電生理記錄過程：

繼代細胞後隔日，拿出種有細胞的3.5 cm 細胞培養皿至室溫，用細胞外液沖洗五次，再加入2 ml的細胞外液，放置顯微鏡下，並在室溫(~22℃)下進行全細胞電壓箝制(whole-cell patch clamp)電生

理之測量。

首先，加入細胞內液至微細玻璃管電極（電阻為4-7 MΩ）內，再以微細玻璃管電極附上細胞膜，進行封口，並進一步產生全細胞電流測量模式。利用電壓箝制放大器(EPC-10 amplifier, HEKA Electronik, Lambrecht, Germany)和Pulse 8.60來記錄全細胞電流變化；而過濾是2 kHz，收集實驗結果頻率是10 kHz，再用Pulsefit 8.60(HEKA Electronik, Lambrecht, Germany)軟體分析結果。因電極同時負責偵測細胞膜電位，並使電壓可箝制在設定之數值中，而N2A細胞及PC-12 細胞，其膜電位被固定在-70 mV，再以不同流程去測量，得到實驗結果（請詳見結果之圖例部分）。

三、濃度反應曲線：

以連續+30mV電壓刺激（持續3.5秒，間隔20秒）N2A細胞，再加入不同濃度之HMJ-53A (1、3、6、10、18、30 μM)至N2A細胞，再以連續+30mV電壓刺激，再記錄受HMJ-53A抑制後的穩定（steady-state）Kv電流，並以Hill方程式得到曲線。Hill方程式：$Idrug/Icontrol = 1/\{1+([HMJ\text{-}53A]/K_d)^n\}$，Idrug表示加入HMJ-53A後，記錄到的Kv電流；Icontrol 表示未加入HMJ-53A，獲到的Kv電流，[HMJ-53A]表示加入細胞外液中HMJ-53A的濃度，K_d表分離常數，n表示Hill係數。

四、活化曲線圖及鈍化曲線圖：

Kv通道活化之電壓依賴性，通常使用尾部電流 (tail current)去評估，但是在此實驗中，因加入HMJ-53A後，鈍化速率非常快，所以，用尾部電流去評估是不準確的。因此，用去極化的刺激而得到的Kv電流和傳導性(G)，然後用G = I/V-Vr 評估並得到曲線，而Vr = (RT/zF)ln(Ko/Ki)，V表示實際設定的電壓，Vr表鉀離子反轉電位 (reversal potential)，I是電流，R是氣體常數，T是溫度，z是離子電荷數，而鉀離子為+1 ，F表法拉第常數 (Faraday constant)，Ko和Ki分別代表為細胞外液及微細玻璃管電極內之細胞內液的鉀離子濃度。活化之電壓依賴性結果，可用波茲曼方程式 (Boltzmann equation)得到活化曲線，$G/Gmax = 1/\{1+\exp[(V_{1/2} - V)/k]\}$來描述通道開或關的機率與細胞膜電位之間的關係。$V_{1/2}$代表全部通道打開一半時的細胞膜電位，k值是斜率 (slope factor)，代表通道之開關對於細胞膜電位變化之依賴程度。

五、穩定狀態之鈍化 (Steady-state inactivation)曲線：

由 $I/Imax = 1/\{1+\exp[(V - V_{1/2})/k]\}$ 得之，$V_{1/2}$ 表示全部通道打開後，呈現鈍化狀態一半時的細胞膜電位， k 是斜率 (slope factor)，即通道之鈍化對於細胞膜電位變化之依賴程度。

第五節：電生理(Electrophysiology)記錄流程

因每個實驗流程不相同，為了方便閱讀，詳細的流程放置在每個結果之圖例解說中。

第六節：統計方法

結果數據顯示皆以means ± SEM；視實驗情況，用unpaired或paired student's t test 去比較兩組差異，而 $p<0.05$為顯著差異。

第三章：研究結果

第一節：HMJ-53A在N2A細胞外側上作用，並加速慢性鈍化現象

當N2A細胞被去極化，會產生衰退(decay)速度極慢的外電流(Fig.1 A,B)，而這樣的慢性衰退現象可稱之為C型鈍化 (Kurata and Fedida, 2006)。而在此實驗中，給予N2A細胞10分鐘的連續（每一次刺激，間隔20秒）+30mV去極化，測得其電流衰退速度，並無因時間增加而加快衰退速度 (Fig.1 A,B) （衰退 τ 在0秒和600秒，分別為 1440 ± 170 ms 和 1376 ± 164 ms, n = 5）。

在Fig.1C,D中，N2A細胞連續去極化時，在細胞外加入30 μM的HMJ-53A後，意外發現整個衰退速度大幅度的加快，而HMJ-53A影響衰退速度至平衡時，衰退 τ 甚至小於 0.1秒（加入HMJ-53A之衰退 τ = 85.6 ± 7.7 ms，n = 16；未加HMJ-53A之衰退 τ 在0 分鐘 = 1677 ± 120 ms，n = 19；$p < 0.05$）。

而這樣的影響是可逆的，也就是在產生加速衰退後，再以灌流沖洗方式，洗走HMJ-53A，發現經過10至12分鐘的沖洗後，回復到未加HMJ-53A的衰退速度（Fig.1E,F；恢復95.3 ± 16.5 %, n = 4）。

Fig.2中，表示HMJ-53A抑制穩定狀態電流之濃度依賴性。分別以不同濃度1、3、6、10、18 及30 μM的HMJ-53A，看其抑制穩定狀

態電流，其IC_{50}為9.2 μM，並從Hill plot獲得Hill係數為3.5；因此數值非常的高；所以，可得知HMJ-53A作用在N2A細胞之Kv通道，有數個結合位置。

此外，我們在另一細胞株PC-12細胞，去證實HMJ-53A是否在另一株細胞上，也會影響Kv電流之衰退速度；在PC-12細胞，給予連續（每一次間隔20秒）+30 mV去極化，發現未加HMJ-53A (30 μM)，衰退 τ 為762 ± 272 ms，而加HMJ-53A (30 μM)等至作用平衡時，其衰退 τ 加速至77 ± 13 ms ($p<0.05$, $n = 6$)。

更進一步，我們想探討出，到底HMJ-53A針對哪一種Kv通道作用呢？而在N2A細胞轉殖入Kv2.1之cDNA，當測量到已轉殖入Kv2.1 cDNA的N2A細胞之電流（可＞3 nA）後，給予連續（每一次間隔20秒）+30 mV去極化，發現衰退 τ 為4600 ± 130 ms，而加入HMJ-53A (30 μM)等至作用平衡時，其衰退 τ 加速至300 ± 70 ms ($p<0.05$, $n = 3$)。從此結果可得知， HMJ-53A會針對Kv2.1產生加速慢性鈍化現象 (Fig.3)。

從以上結果，讓我們想到究竟HMJ-53A作用在細胞何處呢？而主要作用位置，分為細胞內及細胞外兩大部分；首先探討細胞內作用，在N2A細胞中，在微細玻璃管電極之細胞內液中加入HMJ-53A (30 μM)（表示細胞內加入）後，給予細胞連續（每一次間隔20秒）+30

mV去極化，經過15分鐘後，衰退速度並未改變（衰退 τ：0分鐘和15分鐘分別為1270 ± 151 ms 和 1418 ± 128 ms, n = 4）。隨之於細胞外液中加入（表示細胞外）HMJ-53A (30 μM)後，發現電流衰退速度大幅度增加（於作用平衡，衰退 τ 為 58 ± 6 ms, n = 3）(Fig.4A,B)。

綜合以上結果可確定，HMJ-53A產生加速慢性鈍化現象，是作用於細胞外並非細胞內。

第二節：HMJ-53A作用，是否與蛋白質激酶之磷酸化有關呢？

用產生磷酸化作用的非選擇性蛋白酶抑制劑：Staurosporine (Cogolludo et al., 2003)，去確定HMJ-53A是否因產生磷酸化作用而加速Kv電流衰退。加入Staurosporine (100 nM)於培養皿中，等待30分鐘後，給予N2A細胞連續（每一次間隔20秒）+30 mV去極化，發現並未改變衰退速度；再加入HMJ-53A (30 μM)後，整個大幅度加快其衰退速度。比較已加入HMJ-53A之Staurosporine（已加及未加）兩組比較，發現加入Staurosporine不會改變HMJ-53A對衰退速度之影響 [已加和未加Staurosporine (100 nM)分別為96±7 ms 和 105±9 ms, $p>0.05$, n = 3]。

從上述結果可知，HMJ-53A產生加速慢性鈍化現象，與蛋白質激酶之磷酸化似乎無相關性。

第三節：HMJ-53A作用在Kv通道之關閉階段

接下來要探討HMJ-53A作用在Kv通道之關閉或開啟階段呢？當N2A細胞於全細胞電流測量後，先給予第一次+30 mV去極化並記錄其電流 (Fig.5A)，隨後在細胞外加入 HMJ-53A (30 μM)，並等待4分鐘（4分鐘內，並未給予任何去極化）；而4分鐘後，再給予第二次+30 mV去極化並記錄其電流 (Fig.5B)，再比較這兩次的結果，發現第二次比第一次的高峰電流下降至61.9 ± 5.3 %　($p<0.05$, $n = 4$)。從此結果得知，HMJ-53A阻斷作用於Kv通道之關閉階段，進而以灌流方式將HMJ-53A沖洗走，而其回復至未加HMJ-53A之電流(102.7 ± 3.8 %) (Fig.5C)。

第四節：HMJ-53A並非為通道外孔之直接阻斷劑

HMJ-53A是否為通道外孔之直接阻斷劑呢？已知HMJ-53A作用在細胞外，而作用在細胞外有兩種主要原因，造成Kv通道電流加速衰退，第一個是直接堵住通道外孔上，第二個是使選擇性過濾器倒塌所造成的。

首先要探討的是，當Kv通道開啟時，是否HMJ-53A與通道上的孔洞有親和力呢？假如此假設是正確的，HMJ-53A與通道之間的相關性：在加入HMJ-53A後，會隨著去極化刺激上升，而增加電流衰退速度。於是，我們著手實驗，給予不同程度去極化刺激，在N2A細胞，加入HMJ-53A後，是否會影響電流衰退之速率 (Fig6)。在未加HMJ-53A此組中，給予不同去極化刺激，發現電流衰退速度一致，因給予極端的去極化 (> +70 mV)時，所以會有輕微電流衰退速度減慢現象 (Fig.6A,C)；而在加入HMJ-53A (30 μM)此組中，給予寬廣範圍的去極化(0至+100 mV)，得到的結果顯示，增加衰退的速度幾乎一樣，不會因隨著去極化增加而衰退速度加快 (Fig.6B,C)。從此結果可以反駁以下之假設：加入HMJ-53A後，因增加去極化刺激，而增加HMJ-53A與通道親和力，使電流衰退速度更快。

Fig. 7A表示，在N2A細胞中，加入HMJ-53A (10 μM)（選擇此濃度是因為其可大約阻斷Kv電流一半，見Fig.2）後，穩定狀態之Kv電流的阻斷百分比，不會受不同程度電壓刺激而改變。不禁讓人聯想到，藥物和通道間的親和力與通道開啟程度無相關性。

所以，更進一步去證實HMJ-53A並非直接堵住通道外孔，而造成加速衰退現象。於是，改變細胞內鉀離子濃度去探查是否會影響HMJ-53A作用？假如HMJ-53A直接堵住通道外孔，HMJ-53A與鉀離

子會彼此在孔道上產生衝突。所以，降低細胞內的鉀離子濃度，將會有助HMJ-53A阻斷電流之能力。因此，在此實驗中，降低一半細胞內的鉀離子濃度（從140 mM降至70 mM）【為了維持細胞內滲透壓，所以，加入140 mM 蔗糖(sucrose)】，是否會增加HMJ-53A作用？而從結果得知，在N2A細胞上，對HMJ-53A (10 μM)阻斷Kv電流百分比或是加快C型鈍化現象無影響 (Fig. 7B, C)。

為了更進一步確定HMJ-53A並不是堵住通道外孔而造成加速衰退現象；用TEA來證實，而TEA是普遍使用的Kv通道阻斷劑，其作用是直接堵住通道外孔而阻斷Kv電流 (Hille, 2001)。在此實驗中，從細胞外中加入TEA (3 mM)後，立即抑制Kv電流，但是卻無改變電流衰退速率 (Fig. 8)（衰退 τ，未加TEA之0分鐘和加入TEA後10分鐘，分別為1727 ± 373 ms 和1430 ± 350 ms, n = 3），此結果與HMJ-53A對比出衰退速度完全不同。

所以，綜合以上結果，強烈顯示，HMJ-53A並不是直接堵住通道外孔的。

第五節：HMJ-53A作用在Kv通道之鈍化閥門

由以上結果可知HMJ-53A並非直接堵塞通道外孔作用。因此，HMJ-53A加快電流衰退，有可能是作用在鈍化閥門關閉階段上，並

讓人懷疑是否作用在選擇性過濾器本身上而加快其壓縮，增加C型鈍化速度；換句話說，或許HMJ-53A作用是直接經由增加C型鈍化速度。

更仔細去探討，在N2A細胞上，到底HMJ-53A如何影響Kv通道之鈍化作用；所以，加入HMJ-53A後，觀察Kv電流的穩定狀態之鈍化是否有受影響呢 (Fig. 9A)？在加入HMJ-53A此組，比未加HMJ-53A此組，其穩定狀態之鈍化曲線左移12 mV（未加及已加HMJ-53A，分別為$V_{1/2}$ = -21.2 ± 2.5 mV和-33.0 ± 2.3 mV; $p<0.05$）；不管如何，HMJ-53A並未改變其斜率(未加及已加HMJ-53A，分別為6.9 ± 1.3 and 5.9 ± 1.2；$p>0.05$)。而另一點引人注意，在未加HMJ-53A組別中，鈍化現象在較強烈的去極化下 (> +50 mV)逐漸減慢，此結果稱之為U型鈍化 (U-type inactivation)（Klemic, 2001; Kurata, 2002, 2005），而此鈍化作用，為何在極端的去極化中，會減弱其鈍化作用，現今對於其主要的機制尚未明白。在已加HMJ-53A此組中，已看不到U型鈍化，顯示對鈍化之抗拒作用，已被HMJ-53A克服。這樣的結果可進一步支持HMJ-53A作用在鈍化閥門之假說。

另一方面，HMJ-53A是否會影響鈍化閥門的恢復呢？用dual-pulse方式去檢視有或沒有加入HMJ-53A的Kv電流恢復的情況 (Fig.10)。讓人意外的發現，有否加入HMJ-53A對Kv電流之恢復的速率沒有影

響，兩者皆須要好幾秒才能完全恢復，而恢復速率最佳的fit方式為double-exponential；快速恢復中，未加及已加HMJ-53A τ 分別為187 ± 55 和 142 ± 38 ms (p > 0.05; n= 6-7)，而在慢速恢復中，未加及已加HMJ-53A， τ 分別為3115 ± 982和1542± 810 ms（p > 0.05; n = 6-7）。從這些結果中得知，HMJ-53A加快鈍化閥門關閉的速度，但卻不阻礙其恢復情形。

第六節：HMJ-53A不會影響Kv 通道上之活化閥門

此實驗中，再深入研究，在N2A細胞中，是否HMJ-53A會影響Kv通道中的活化閥門？從電壓依賴曲線圖 (-70mV至+70mV)中，可知Kv通道之活化閥門並無受到HMJ-53A影響 (Fig.9B)（未加及已加HMJ-53A，分別為$V_{1/2}$ = 12.8 ± 3.2 mV和15.2 ± 1.6 mV；p>0.05），並且HMJ-53A也不影響斜率(未加及已加HMJ-53A，分別為11.1 ± 0.5 和 13.9 ± 1.4; p>0.05)。

在Fig.9C中，比較未加及已加HMJ-53A組之活化kinetics，得知並無分別。從Fig.9D的量化曲線圖顯示，Kv電流被更強之去極化刺激時，隨之增加活化速率；已加HMJ-53A組別中，可得知在不同的去極化刺激下，與未加HMJ-53A組別比較並不會改變其活化速率。由以上結果可得知，HMJ-53A不會影響Kv通道之活化閥門。

第七節：HMJ化合物其結構與產生加速鈍化閥門關閉之相關性

綜合以上的結果，得知 HMJ-53A 有選擇性的作用在 Kv 通道上之鈍化閥門，而加速其關閉。在 Fig11 表示數個 HMJ 衍生物，抑制穩定狀態電流之濃度依賴性 (concentration-dependence)。而到底 HMJ 化合物的結構中，到底是哪一個部分(moiety)會造成這樣的作用呢？在此實驗中，假如增加或減短 HMJ-53A 其中的 CH_2CH_3，是否會影響作用的強度？而依 CH_2CH_3 的短長，分別有 HMJ-1、HMJ-29A、HMJ-53A 及 HMJ-73A（見圖 A、B）。

在記錄 N2A 電流時，給予連續去極化+30mV，加入 HMJ-1 (30 μM)，並無抑制穩定狀態之電流。再進一步證實，在 N2A 細胞上，給予連續去極化+30mV，再加入不同濃度之其它 HMJ 化合物，而看其對穩定狀態電流之影響。得之 HMJ-29A 之 IC_{50} 為 17.5 μM，並從 Hill plot 獲得 Hill 係數為 2.3。HMJ-53A 結果見 Fig2。HMJ-73A 之 IC_{50} 為 6.5 μM，Hill 係數為 1.9。

從以上結果得知 HMJ-1 不影響 Kv 電流。而 HMJ-29A 為中度影響 Kv 電流，HMJ-53A 及 HMJ-73A 為強度影響 Kv 電流 (Fig. 11)。所以，綜合以上結果，與我們的假設符合，可以得知 HMJ-53A 的結構中，CH_2CH_3 為主要影響鈍化閥門的關閉加速之結構。

第四章：討論

Kv 通道之 C 型（慢性）鈍化現象的分子機制作用，目前並不是完全了解，而現今已知其作用機制為：Kv 通道上的選擇性過濾器或是其附近位置被壓縮，而導致孔洞變小，而使鉀離子無法順利通過孔洞 (Kurata and Fedida, 2006；Hille, 2001)。而在藥理學中，作用於 C 型（慢性）鈍化閥門之探針藥是很重要的。C 型（慢性）鈍化現象，調節神經細胞的興奮性並產生動作電位之輪廓及頻率，是非常重要；但是，至目前為止，特定針對於 C 型（慢性）鈍化現象之機制探討的藥物是很缺乏的。

所以，在此研究中發現在N2A (neuroblastoma)細胞上，HMJ-53A能加速Kv電流慢性鈍化現象。我們證實 HMJ-53A在N2A細胞中Kv通道產生此作用，是在細胞外並非細胞內 (Fig.4)。而Fig.5之結果，可以是由於兩種可能性：第一個，HMJ-53A之作用是在Kv通道關閉階段；第二個，HMJ-53A之作用是在Kv通道開啟階段。假設作用於開啟階段時，當HMJ-53A作用在Kv通道上時，會造成活化速率變慢，且足以阻礙防止電流至最高峰。但從結果上可知，不可能為後者的假設，因為從Fig.9C,D可知，活化kinetics並不會受到HMJ-53A的影響。

在Fig.5的結果上說明，假設當通道剛開啟，HMJ-53A直接堵住通

道上外孔，並部分重疊正在活化的電流；對於這樣的想法，需提出的一個假設為：第一階段，HMJ-53A快速地直接堵住孔洞，且在一開始活化後非常快速的堵住孔洞，而之後第二階段中，在細胞持續極化情況下，相對以緩慢的速度繼續接近其結合位置，隨之產生越明顯的電流下降情形。假如前述的第二個階段存在，很有可能表示有一個drug-channel結合的位置，而此位置是靠去極化（或通道打開）才暴露出來的。

所以，在我們的研究中去進一步探討，HMJ-53A與通道相互作用，是否與各種不同程度的去極化有關呢？然而，當有HMJ-53A作用時，在不同程度的去極化下，電流衰退的速度是不變的 (Fig. 6)。再者，HMJ-53A抑制Kv電流的百分比也是非電壓依賴性的 (Fig.7A)。還有，假如HMJ-53A直接堵住通道上孔洞，則將會與鉀離子在通道之孔洞內相遇；假如降低細胞內鉀離子濃度，HMJ-53A將會更強地阻礙鉀離子的流出。然而，從結果中得知，HMJ-53A (10 μM)對於抑制Kv電流的百分比或加速C型鈍化，皆不因為大幅度降低細胞內鉀離子濃度而受影響 (Fig.7B,C)。

由以上我們的結果可知，HMJ-53A的作用不太可能是直接堵塞通道洞孔所造成的；這樣的結果更能顯示HMJ-53A作用在鈍化閥門。可讓我們想像，當Kv通道在關閉狀態，HMJ-53A已經鈍化通道，因

此讓我們得知，HMJ-53A阻斷Kv通道是在關閉狀態，當Kv通道打開後，HMJ-53A加速鈍化閥門的關閉。

在*Shaker* (Kv1)通道及一些哺乳類動物相似*Shaker*之通道中，提升細胞外鉀離子濃度和從細胞外加入TEA，會阻礙C型鈍化 (Choi et al., 1991; Fedida et al., 1999; Lopez-Barneo et al., 1993; Molina et al., 1997)。無論如何，在N2A細胞上，Kv通道中的C型鈍化速率，並不會受到TEA (3 mM)的影響 (Fig. 8)。這樣的結果，或許是因為在N2A細胞中，並無哺乳類動物相似*Shaker*之通道存在。而在我們實驗中，則顯示HMJ-53A能作用於Kv2.1，而加速C型鈍化 (Fig. 3)。

但是有趣的是，HMJ-53A不會使Kv通道回復的速率減慢 (Fig. 10)，這也表示，在復極化階段，HMJ-53A非常快速的離開Kv通道。基於HMJ-53A抑制電流的Hill 係數3.5 (Fig.2)，表示HMJ-53A在Kv通道上，有數個結合位置；因此我們提出一個觀點，在Kv通道上，HMJ-53A作用於某一個結合位置，而產生closed channel block，而HMJ-53A作用於其他結合位置，而加速慢性鈍化。所以，在復極化期間，HMJ-53A離開後者之結合位置比較快，而不減慢及影響通道的恢復時間。

關於HMJ-53A與鈍化閥門之間的相互作用，HMJ-53A導致穩定狀態之鈍化曲線左移12 mV。在未有HMJ-53A的N2A細胞上，可以記

錄一個明顯的U型鈍化之Kv電流。因此，在較強的去極化中 (> +50 mV)，鈍化閥門不容易關閉。有文獻指出，Kv1.5、Kv2.1和Kv3.1，會表現U型鈍化 (Klemic et al., 2001; Kurata et al., 2005; Kurata et al., 2002)；這或許表示N2A細胞中，存有一個或著一些這樣的通道，才產生這樣的U型鈍化。

在極端的去極化下，Kv通道難以鈍化，而因此表現之U型鈍化，其分子機制至今還不清楚。而HMJ-53A能克服此U型鈍化 (Fig. 9A)，更能證明HMJ-53A能加劇鈍化閥門的關閉。

HMJ-53A是否能影響細胞質內的活化閥門作用呢？在此我們提供了證據，去顯示HMJ-53A對於Kv通道上活化的電壓依賴性和kinetics並不影響 (Fig. 9B – D)。綜合以上結果，作用於Kv通道的鈍化閥門的HMJ-53A是一個新穎的藥物。

目前已有幾篇報導指出，有幾種化合物可以增加鈍化閥門速度。KN-93是目前已知作用在細胞外，而能提升Kv通道上慢性鈍化的速度 (Ledoux et al., 1999; Rezazadeh et al., 2006)；但此藥物的作用及影響，沒有完全之可逆性且會作用在活化閥門：活化曲線有輕微的左移現象，並且Boltzmann斜率有明顯的下降。 (Rezazadeh et al., 2006)。而亞麻油酸 (Linoleic acid)也能在Kv1.5和Kv2.1中，加速慢性鈍化，而其作用在細胞外而非細胞內 (McKay and Worley, 2001)；

況且，亞麻油酸會影響活化閥門，使活化曲線左移和加速活化 kinetics (McKay and Worley, 2001)。因此，在我們的研究中發現，HMJ-53A的作用是完全可逆的和有選擇性的作用在鈍化閥門上的。故在往後的研究中，HMJ-53A將可以作為深入探討Kv通道之鈍化閥門之理想藥物。

Quinidine目前已知能導致C型鈍化加速 (Wang et al., 2003)，但quinidine此作用須經由細胞內allosteric的動作且須通道先開啟而才能把電流阻斷。此外，4-aminopyridine是一個作用在細胞質內的Kv通道阻斷劑，但卻被證實出能抑制*Shaker*通道之C型鈍化，但其機轉不甚清楚 (Claydon et al., 2007)。

最後，我們要問的，是否HMJ-53A可作用在細胞膜上或細胞內而激發蛋白質激酶，進而影響鈍化閥門？從我們的結果得知，加入staurosporine至N2A細胞後，不會改變細胞本身的電流衰退，或者也不影響加入HMJ-53A後的C型鈍化速度。而這些否定的結果可以讓我們確定HMJ-53A並不是作用在細胞膜上而再經由某些磷酸化訊息傳遞路徑，去調控C型鈍化。而從HMJ-53A不能在細胞內影響Kv電流的實驗中，意味著HMJ-53A的作用，並不是經由調控細胞內的因子或是擾亂細胞膜上脂質(lipid)的平衡而造成的 (Oliver et al., 2004)。

往後之研究方向，我們想繼續探討在 HMJ 系列衍生物的結構上，大幅度地加長 CH_2CH_3，看其能否加倍增強鈍化之能力？我們也想深入探討 HMJ 衍生物，對於其它已知存在神經細胞上之 Kv 通道，例如：Kv1.1 或 Kv1.2…等之影響 (Sheng et al., 1993; Sheng et al., 1994; Shimada et al., 2007)。另一方面，當 HMJ-53A 在高濃度情況下（例如：100μM），是否會對 Kv 通道上之其它動作有影響，而在 HEK 細胞株上表達 Kv4.3，去深入探討是否高濃度的 HMJ-53A 會影響 Kv 通道上之 N 型鈍化呢？

我們想再深入研究一個有趣的問題，在生理層面，當神經細胞受損時，例如：神經退化疾病；此 HMJ 衍生物其是否有神經保護之功能呢？而作為一種神經保護嶄新之用藥呢？這是往後我們想再深入探討之方向。

第五章：結果圖表與說明

Fig. 1：HMJ-53A 加速 N2A 細胞 Kv 電流慢性鈍化現象

N2A細胞的holding potential是-70mV，連續給予+30 mV去極化刺激（持續3.5秒，間隔時間為20秒）。從結果中每一次刺激的電流最高往最低點fit位置，而得到衰退 τ。

(A)典型的K^+ 電流外流曲線，被+30mV去極化引起，分別於0秒和經過600秒後，且未加任何藥物。

(B) 衰退時間常數從(A)圖得之，每個時間點被plot出 。

(C)典型的K^+ 電流外流曲線，被+30 mV引起，加入HMJ-53A (30 μM)之前後之記錄。

(D)衰退時間常數從(C)圖得之，於未加及已加HMJ-53A(30 μM)後之每個時間點plot出。

(E)典型的K^+ 電流外流曲線，被+30 mV引起，記錄於未加及已加HMJ-53A(30 μM)，和從細胞外沖洗走HMJ-53A後，得之的曲線。

(F)衰退時間常數從(E)圖得之，於未加、已加及沖洗走HMJ-53A (30 μM)之每個時間點plot出。

以上實驗得到的結果，可重複次數皆多於三個細胞以上。

Fig. 1

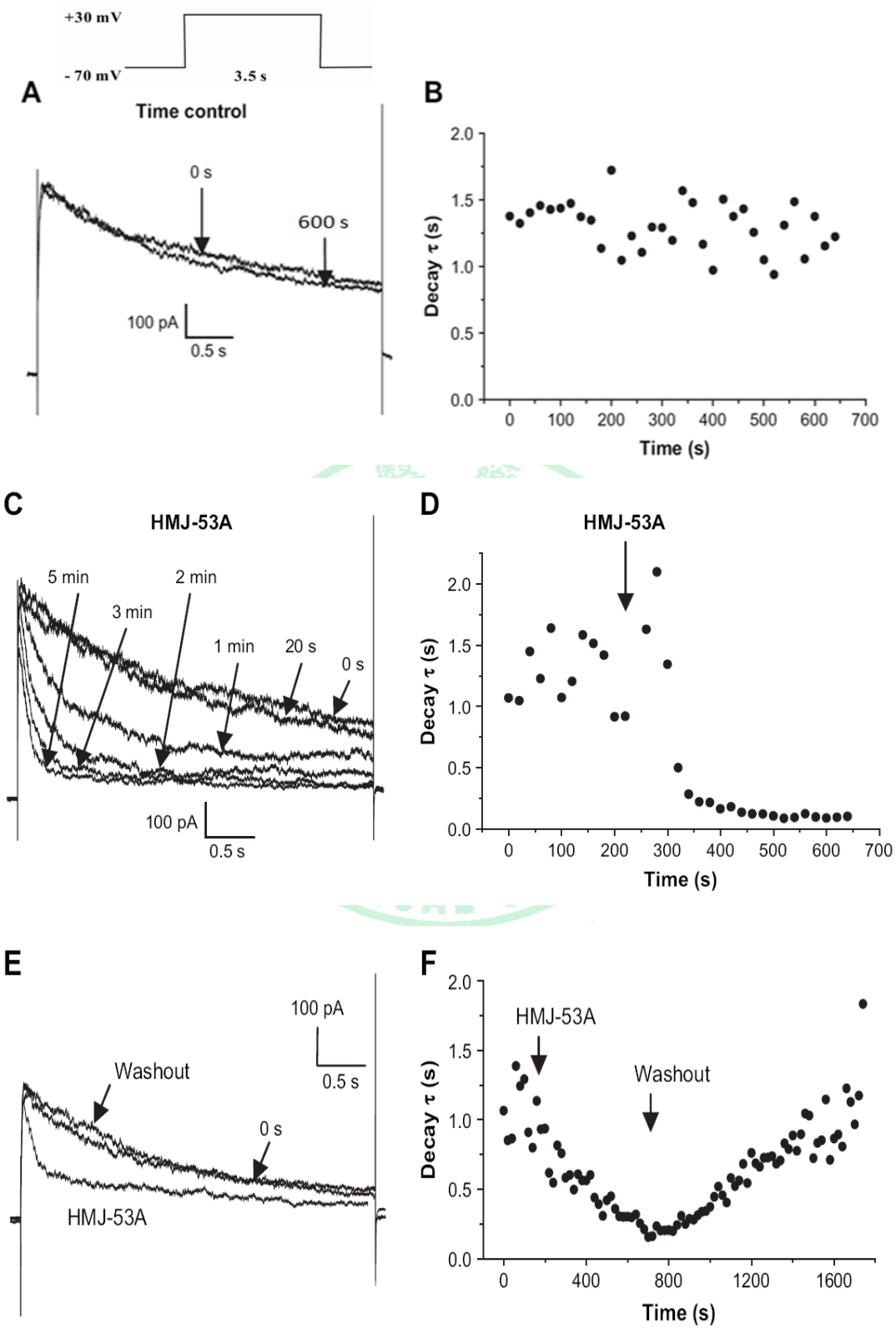
+30 mV
- 70 mV
3.5 s
A
Time control
0 s
600 s
100 pA
0.5 s
B
Decay τ (s)
Time (s)
C
HMJ-53A
5 min
3 min
2 min
1 min
20 s
0 s
100 pA
0.5 s
D
HMJ-53A
Decay τ (s)
Time (s)
E
100 pA
0.5 s
Washout
0 s
HMJ-53A
F
HMJ-53A
Washout
Decay τ (s)
Time (s)

Fig. 2：HMJ-53A 抑制 Kv 電流濃度依賴曲線

細胞的 holding potential 為-70mV，連續給予+30mV 去極化刺（持續 3.5 秒，間隔時間為 20 秒）。再加入不同濃度的 HMJ-53A （3、6、10、18 及 30 μM），並給予同樣的刺激，記錄穩定狀態之 Kv 電流。

把標準化之穩定狀態電流（已加藥/未加藥），作 Y-軸，並把 HMJ-53A 之濃度作 X-軸。

曲線用 Hill 方程式 fit 之。結果為 mean ± SEM，從 3 至 6 個細胞得之。

Fig. 2

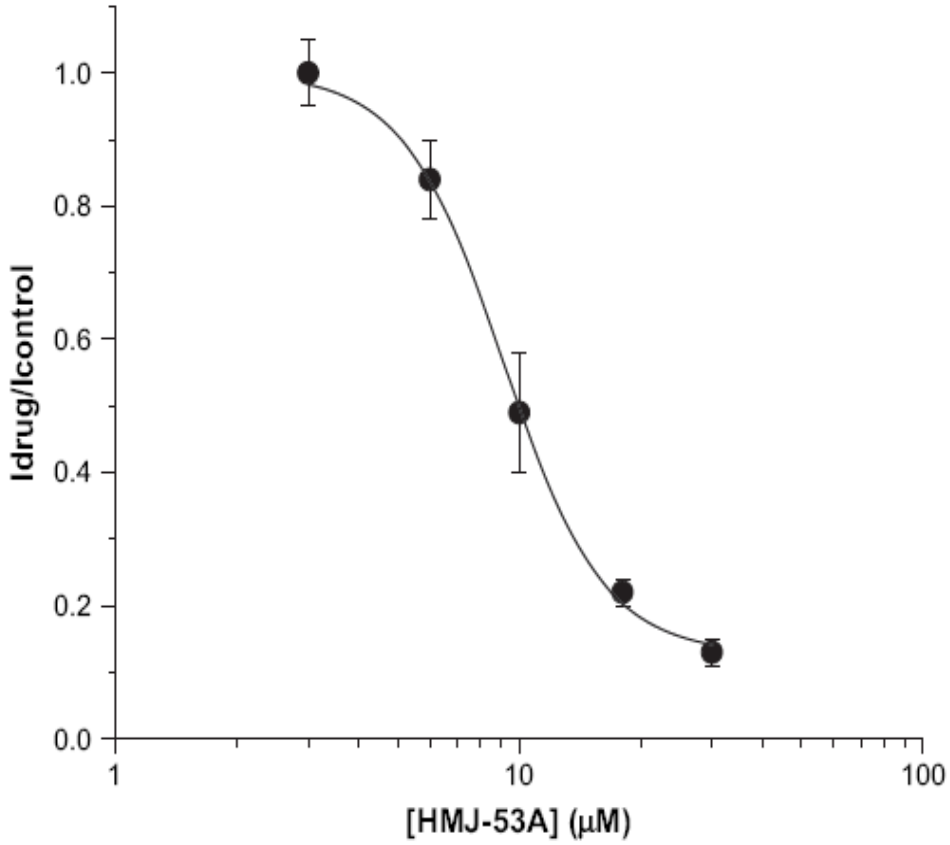

Fig. 3：HMJ-53A 在轉殖 Kv2.1 後之 N2A 細胞上，加速 Kv 電流慢性鈍化現象

在已轉殖 Kv2.1 之 N2A 細胞，holding potential 為-70 mV，給予連續+30 mV 去極化刺激（持續 3.5 秒，間隔時間為 20 秒）。得到 K v2.1 電流，再加入 HMJ-53A (30 μM)。曲線分別為未加藥及加藥後 12 分鐘。

以上實驗得到的結果，可重複於三個細胞上。

Fig. 3

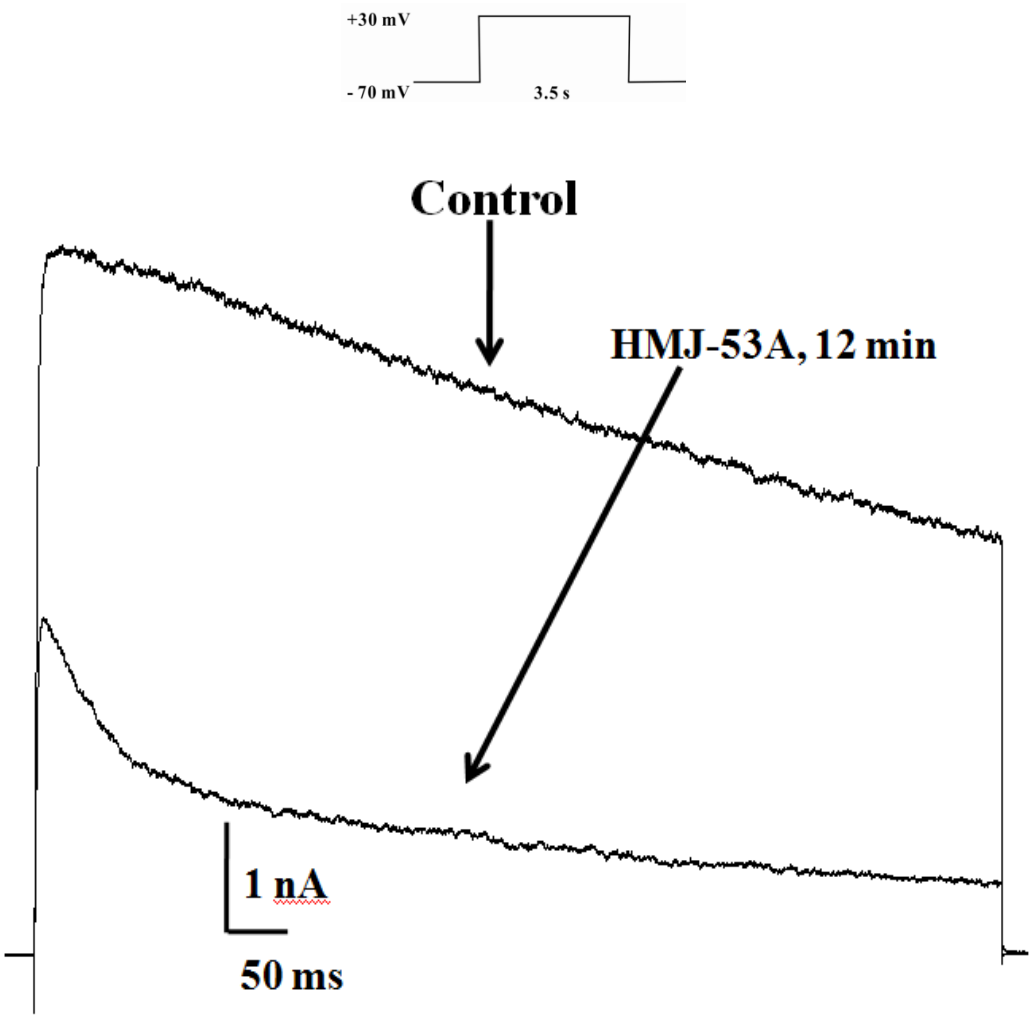

Fig. 4：從 N2A 細胞內加入 HMJ-53A 並不影響 Kv 電流之慢性鈍化

(A) 在微細玻璃管電極之細胞內液中（細胞內）加入HMJ-53A (30 μM)。細胞的 holding potential是-70 mV，給予連續+30 mV去極化刺激（持續3.5秒，間隔時間為20秒）。得到典型的K^+ 電流外流曲線，從0 分鐘至15 分鐘記錄。

再從細胞外，加入HMJ-53A (30 μM)，皆在同一個N2A細胞上進行，得之曲線。

(B) 從結果中每一次刺激的電流最高往最低點fit，而得到衰退 τ。衰退時間常數從(A)圖得之，於未加及已加HMJ-53A (30 μM)之每個時間點plot出。

以上實驗得到的結果，可重複於三個細胞上。

Fig. 4

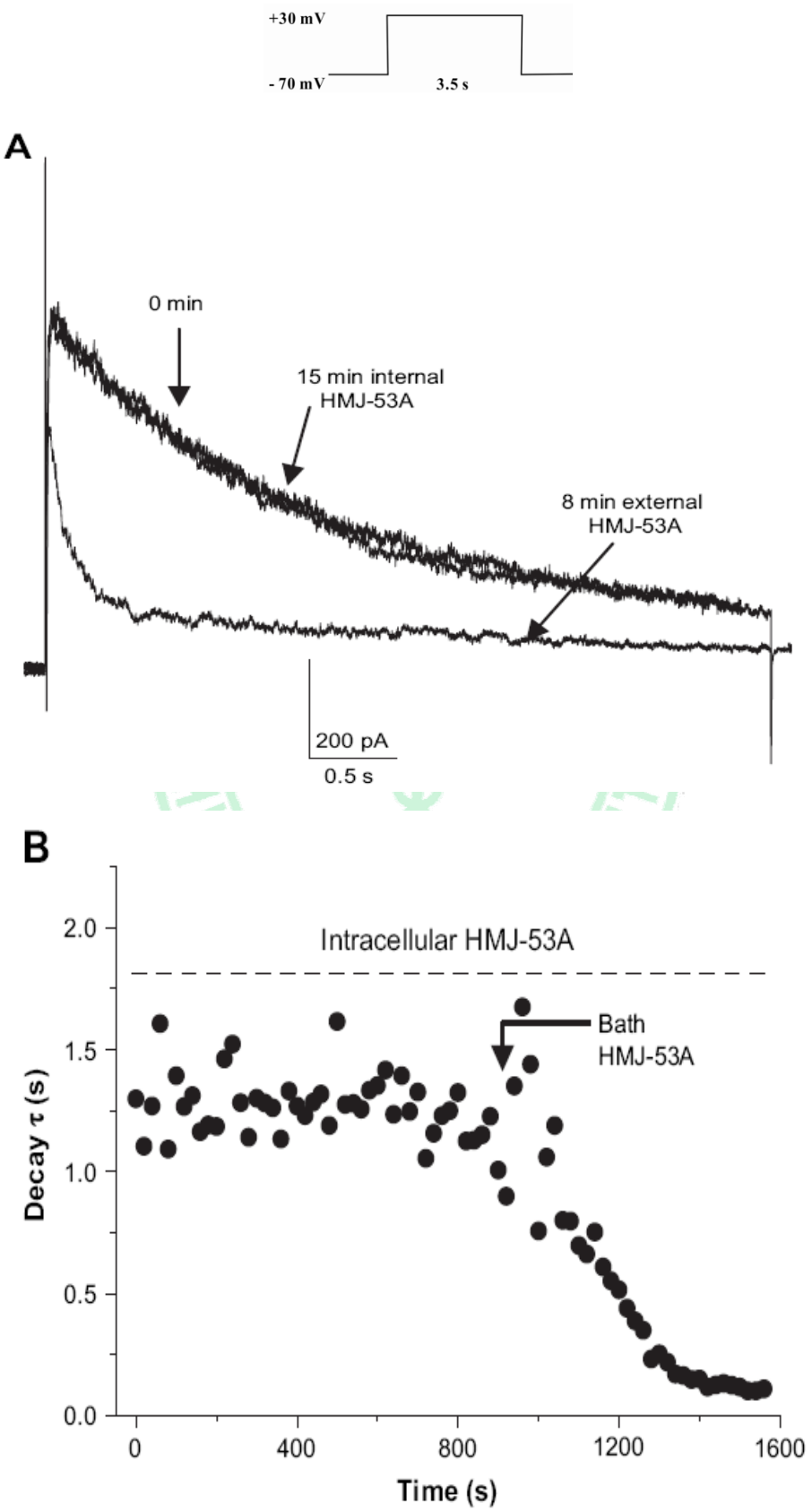
+30 mV
- 70 mV
3.5 s
A
0 min
15 min internal
HMJ-53A
8 min external
HMJ-53A
200 pA
0.5 s
B
Intracellular HMJ-53A
Bath
HMJ-53A
Decay τ (s)
2.0
1.5
1.0
0.5
0.0
0
400
800
1200
1600
Time (s)

Fig. 5：HMJ-53A作用於N2A細胞之Kv通道之關閉階段：

(A) 細胞的holding potential為-70 mV，給予第一次+30mV去極化，得之曲線。隨後給予此細胞HMJ-53A (30 μM)，等待4分鐘，並此期間未給予任何去極化刺激。

(B) 此細胞給予第二次+30mV去極化，並記錄其曲線。

(C) 以灌流方式，從細胞外沖洗走HMJ-53A，並連續（持續3.5秒，間隔時間為20秒）給予+30mV去極化並記錄其曲線。

以上實驗得到的結果，可重複在多於三個細胞以上。

Fig. 5

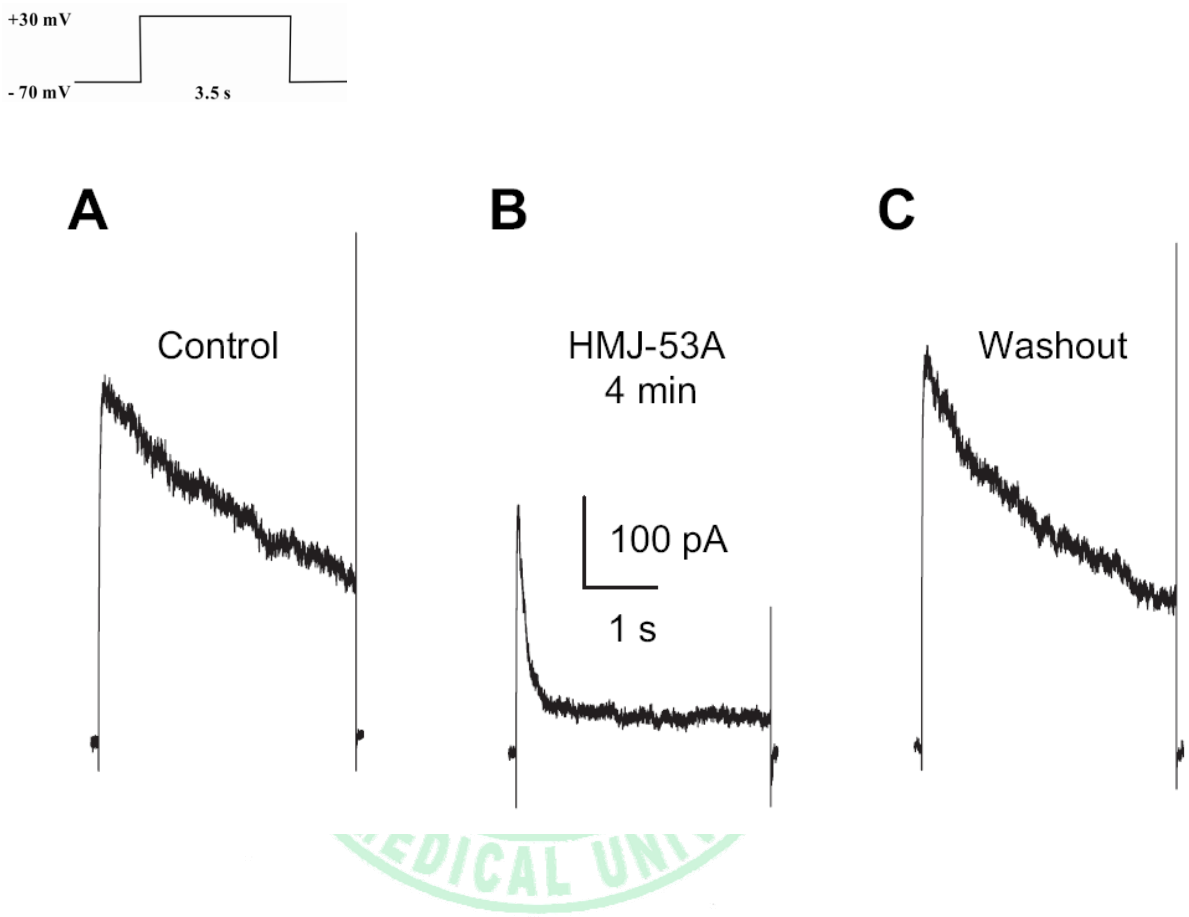

Fig. 6：HMJ-53A加劇電流之衰退，沒有電壓依賴性

(A) 細胞的holding potential為-70 mV，開始給予刺激，一次持續10 s，間隔10秒，每增加10 mV刺激一次，至+100 mV為止，停止刺激。得到典型的K^+ 電流外流曲線，被不同的電壓去極化引起。

(B) 加入HMJ-53A (30 μM)，經過15分鐘後；同(A)刺激方式，測量記錄曲線。得到典型的K^+ 電流外流曲線，被不同的電壓去極化引起。

(C) 從每一次刺激的電流之最高往最低點fit之，而得到衰退 τ。衰退時間常數根據每個不同的去極化電壓plot出。

每一組結果的mean ± SEM，從4個細胞中得到。

Fig. 6

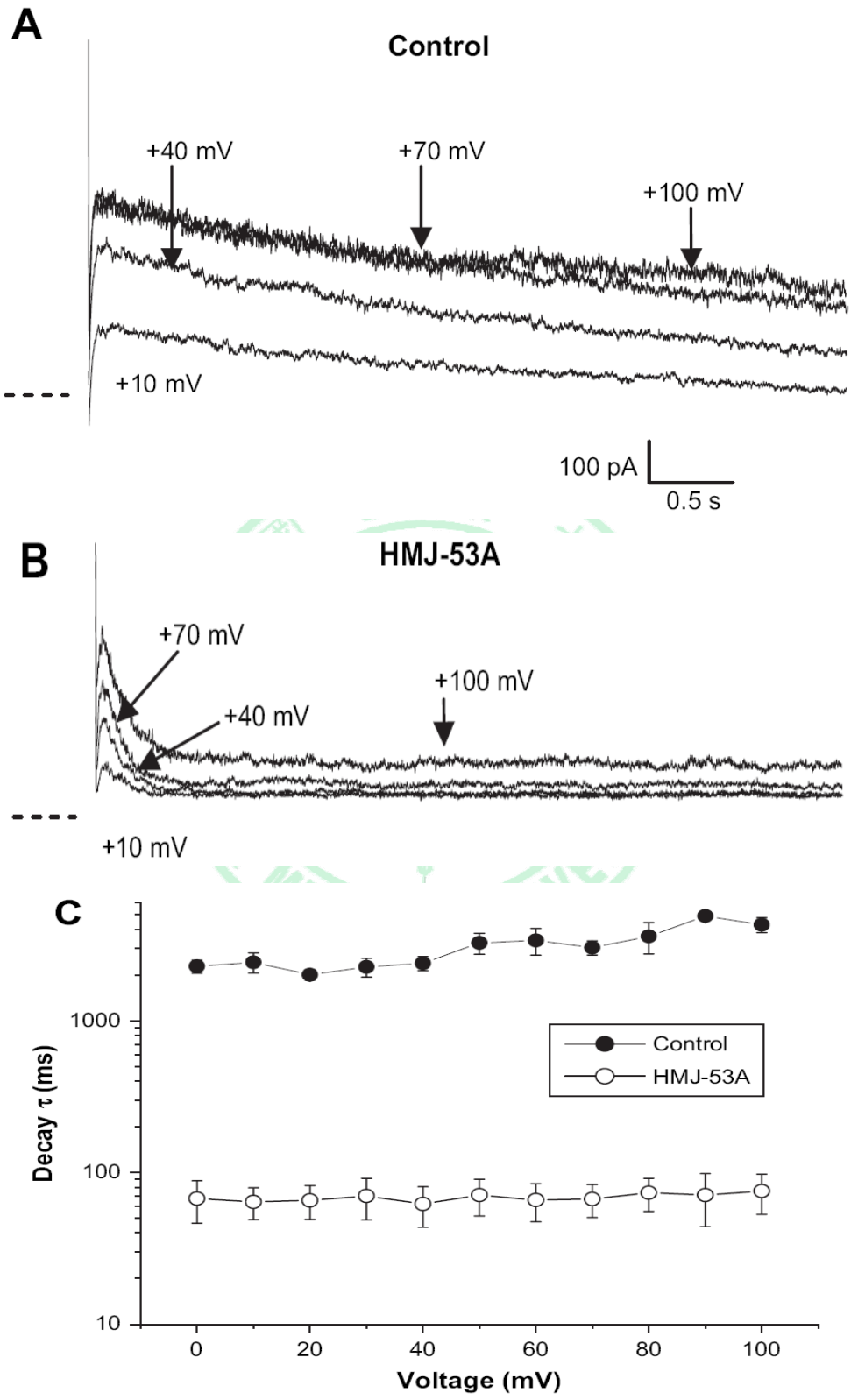
A
Control
+40 mV
+70 mV
+100 mV
+10 mV
100 pA
0.5 s
B
HMJ-53A
+70 mV
+40 mV
+100 mV
+10 mV
C
Decay τ (ms)
1000
100
10
0
20
40
60
80
100
Voltage (mV)
Control
HMJ-53A

Fig. 7：HMJ-53A 阻斷 Kv 電流之強度不受電壓與細胞內鉀離子濃度影響

(A)HMJ-53A (10 μM)阻斷穩定狀態 Kv 電流之百分比，根據每個不同的電壓下 plot 出。

細胞的 holding potential 為-70mV，開始給予刺激（一次持續 10 秒，間隔 10 秒），每增加 10mV 刺激一次，至+100mV 為止，停止刺激。再比較兩組其每個電壓中抑制的電流百分比（已加藥/未加藥電流）×100%，所得到此曲線。

(B)HMJ-53A (10 μM)阻斷穩定狀態之Kv電流百分比。

兩組：微細玻璃管電極內（表示細胞內）鉀離子濃度分別為140 mM 和70 mM，細胞的 holding potential為-70mV，給予連續+30 mV去極化刺激（一個刺激持續3.5秒，間隔時間20秒）。抑制的電流其百分比（已加藥/未加藥電流）×100%，再比較兩組的差異。

(C)在細胞內鉀離子濃度分別為 70 和 140 mM 時，Kv 電流的衰退時間常數 [以加及未加 HMJ-53A (10 μM)]。

微細玻璃管電極內（表示細胞內）鉀離子濃度分別為140 mM和70 mM。細胞的 holding potential是-70mV，給予連續+30 mV去

極化刺激，（一個刺激持續3.5秒，間隔時間為20秒）。再分為未加及已加HMJ-53A(10 μM)兩大組，從結果中的電流最高至最低點fit之，而得到衰退 τ。

每一組結果之mean ± SEM，從4至5個細胞中得到。

Fig. 7

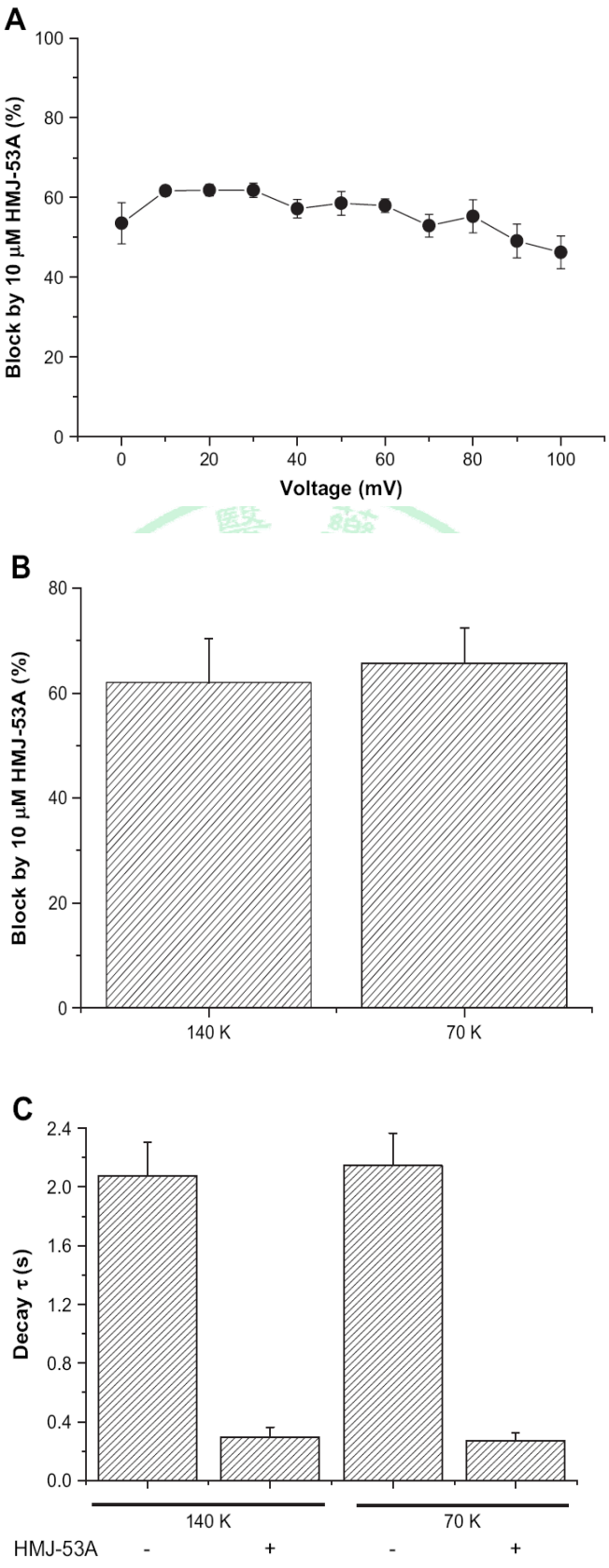
A
Block by 10 μM HMJ-53A (%)
100
80
60
40
20
0
0
20
40
60
80
100
Voltage (mV)
B
Block by 10 μM HMJ-53A (%)
80
60
40
20
0
140 K
70 K
C
Decay τ (s)
2.4
2.0
1.6
1.2
0.8
0.4
0.0
140 K
70 K
HMJ-53A
-
+
-
+

Fig.8：TEA對電流衰退之影響與HMJ-53A不同

(A) 細胞的holding potential為-70 mV，給予連續+30 mV去極化刺激，（一個刺激持續3.5 秒，間隔時間為20秒）。得到典型的K^+ 電流外流曲線，再加入TEA (3 mM)（20秒和600秒後）。

(B) 衰退時間常數：比較未加及已加TEA (3 mM)的結果。於電流最高至最低點fit之，為於每個時間點之衰退 τ。

以上實驗得到的結果，可重複於三個細胞上。

Fig.8

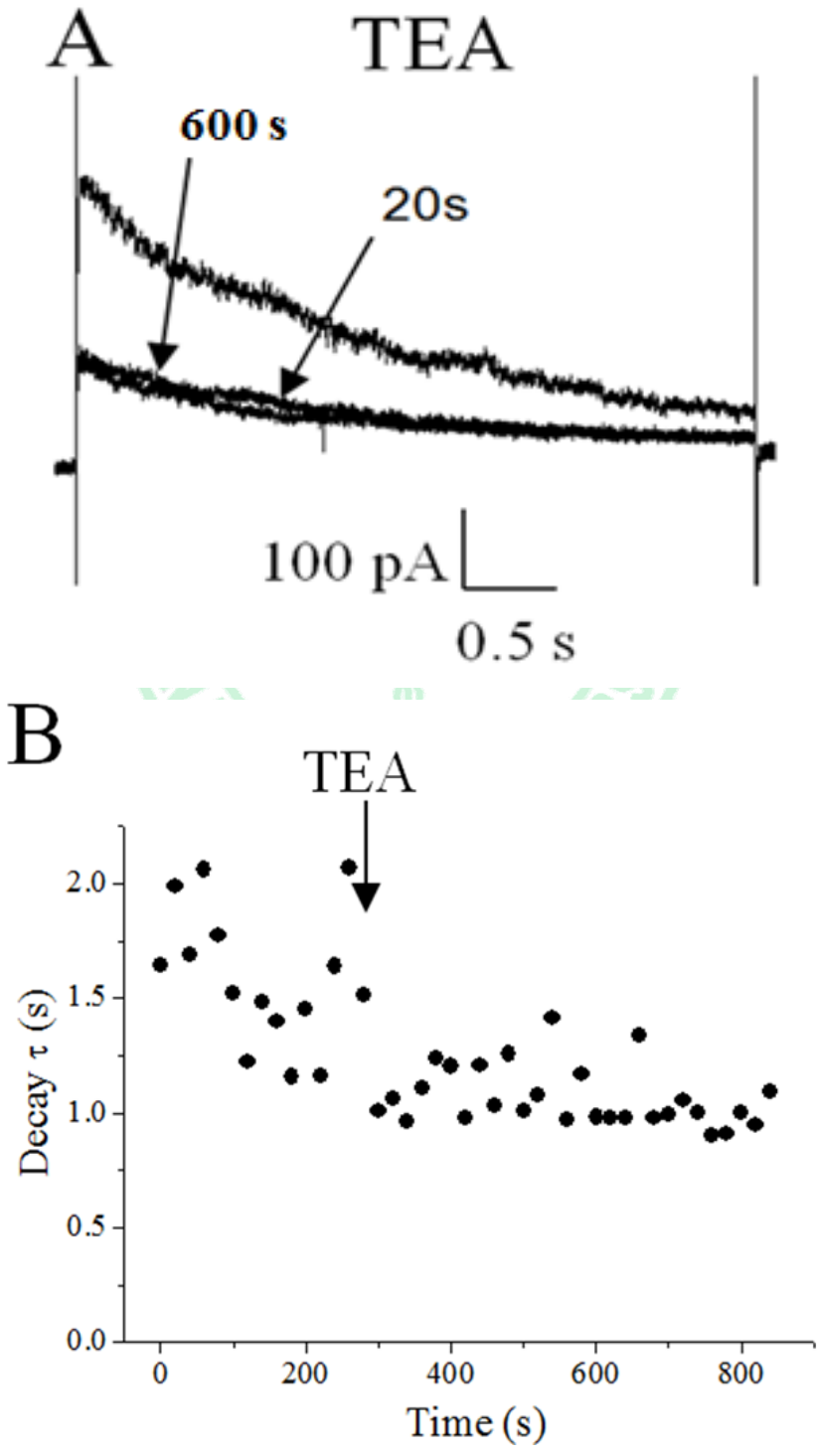
A
TEA
600 s
20s
100 pA
0.5 s
B
TEA
Decay τ (s)
2.0
1.5
1.0
0.5
0.0
0
200
400
600
800
Time (s)

Fig. 9：HMJ-53A 使穩定狀態之鈍化曲線左移

但不影響活化閥門

(A)已加及未加HMJ-53A (30 μM)之N2A細胞中，進行Kv通道電流測量，得之穩定狀態之鈍化曲線。在此實驗使用dual-pulse流程（給予一次pre-pulse，再給予第二次短的pulse）做測量。

細胞的holding potential是-70 mV，先給予pre-pulse刺激（持續10 s），再給予一個+70 mV的test pulse。休息10秒後，接著下一個dual-pulse刺激 （於pre-pulse，每次增加10 mV），刺激至pre-pulse為+100 mV，停止刺激。

而test pulse電流與最大之test pulse電流作標準化，兩組曲線比較其差異。因為在對照組產生‘‘U型鈍化’’現象，所以只從-80至+50mV fit（Boltzmann方程式）。結果之mean ± SEM從每組中4個細胞中得之。

(B)活化電壓依賴性：Kv 電流被不同電壓去極化刺激，而這些不同的電壓，從holding potential為-70mV開始，每增加10mV刺激一次（一次持續0.5秒，間隔2秒），至+70mV止。

Conductances (G)（conductance計算於材料方法中說明）在對照組和加入HMJ-53A 組中，分別與各自最大的conductance

(Gmax)作標準化，在不同的去極化刺激下plot出結果。而此曲線是以Boltzmann方程式去fit之。結果之mean ± SEM從每組中6個細胞中得之。

(C)較早階段的電流traces代表活化之kinetics。細胞的holding potential為-70mV，給予連續+30 mV去極化刺激（一個刺激持續3.5 秒，間隔時間20秒），再加入HMJ-53A。而標準化這兩組並重疊其電流，來比較未加及已加HMJ-53A這兩組。

(D)同(C)之刺激方式，活化時間常數乃於電流上升階段作exponential fit，於不同的去極化電壓，再plot出結果。而得到兩組（未加及已加HMJ-53A）的活化曲線。

每組結果的mean ± SEM，從6至8個細胞中得到。

Fig. 9

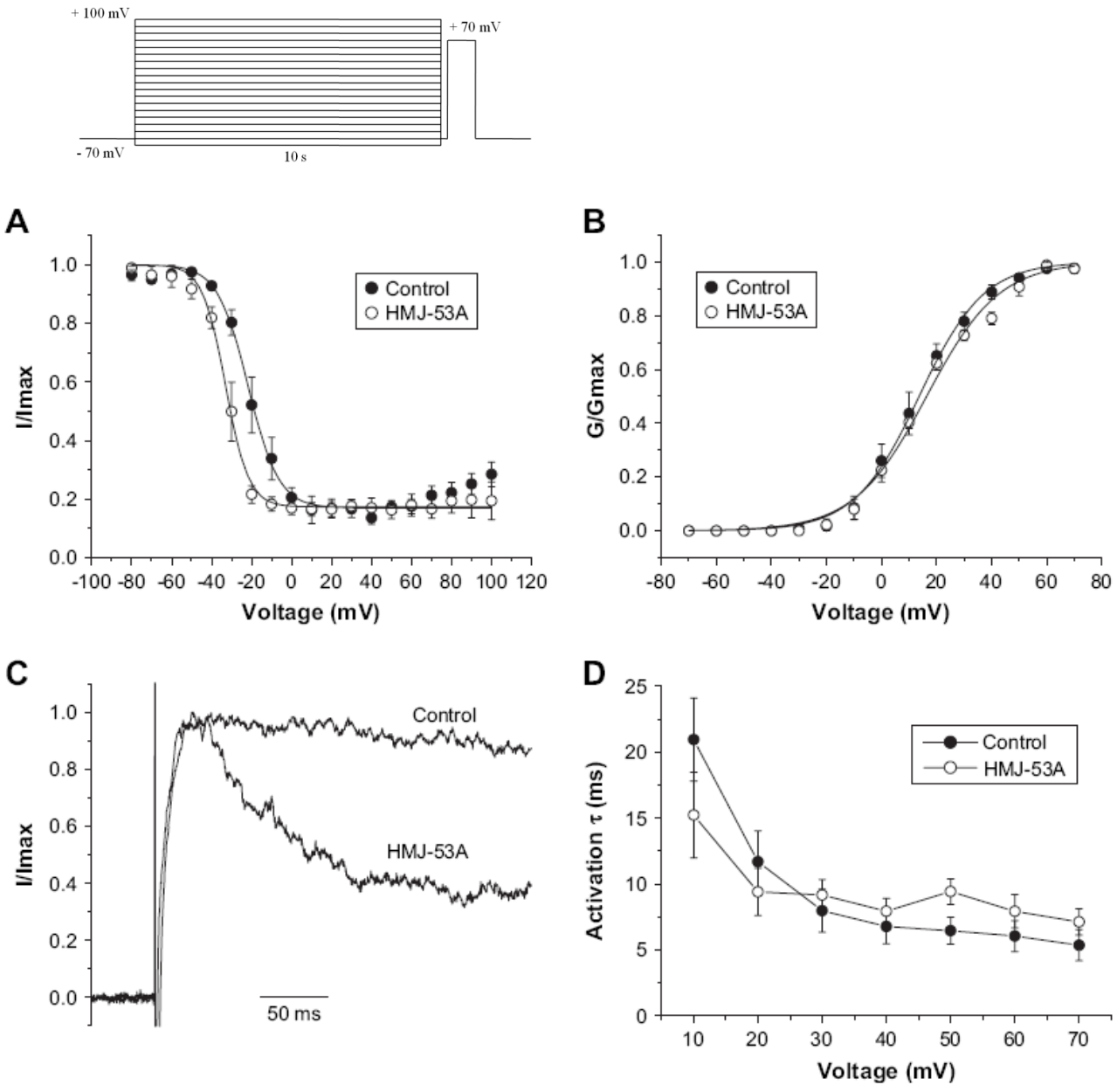
+ 100 mV
+ 70 mV
- 70 mV
10 s
A
I/Imax
Voltage (mV)
Control
HMJ-53A
B
G/Gmax
Voltage (mV)
Control
HMJ-53A
C
I/Imax
Control
HMJ-53A
50 ms
D
Activation τ (ms)
Voltage (mV)
Control
HMJ-53A

Fig. 10：HMJ-53A不影響Kv電流之恢復

電流恢復實驗於N2A細胞中進行，用dual-pulse 流程，細胞的holding potential為-70 mV，給予第一次pulse（+30 mV，持續5秒），然後第二次pulse（+30 mV，持續200 ms）；第一次pulse與第二次pulse間隔時間不同。

把第二個電流 (I2)與第一個電流 (I1)的最大值作標準化(I2/I1)。再把此標準化結果根據不同之時間間隔而plot之。而此曲線用double-exponential功能去fit。

兩組的結果的mean ± SEM，從每組中4個細胞中得到。

Fig. 10

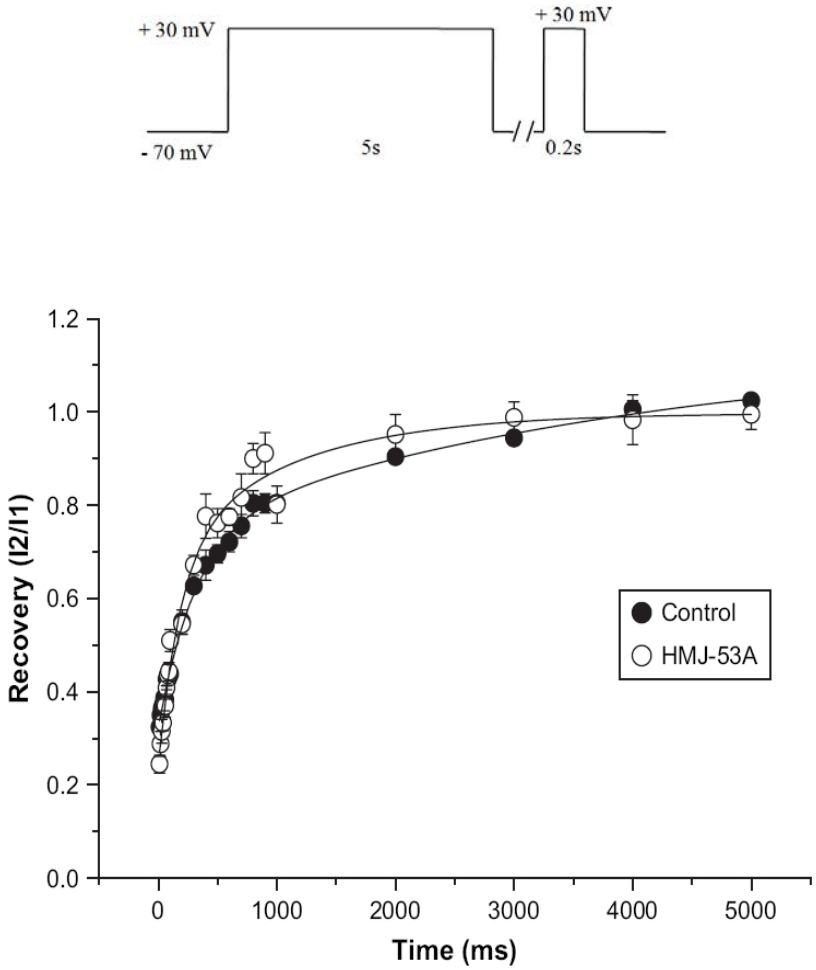

Fig. 11：HMJ衍生物抑制Kv電流之濃度依賴性曲線

N2A細胞holding potential為-70 mV，給予連續+30 mV去極化刺激（持續3.5秒，間隔時間20秒）。再加入HMJ-1 (30 μM)，得之電流，與未加入HMJ-1最大的穩定狀態電流作標準化，再plot出此點。

同上刺激方式，分別加入不同濃度（3、6、10、18 及 30 μM）之其它 HMJ 衍生物，得到之最大的穩定狀態電流與未加入 HMJ 衍生物之最大的穩定狀態電流作標準化（Idrug/Icontrol），並依藥物之濃度作 X 軸而 plot 之，曲線用 Hill 方程式 fit 之。

每組的結果 mean ± SEM，從 3 至 6 個細胞得之。

Fig. 11

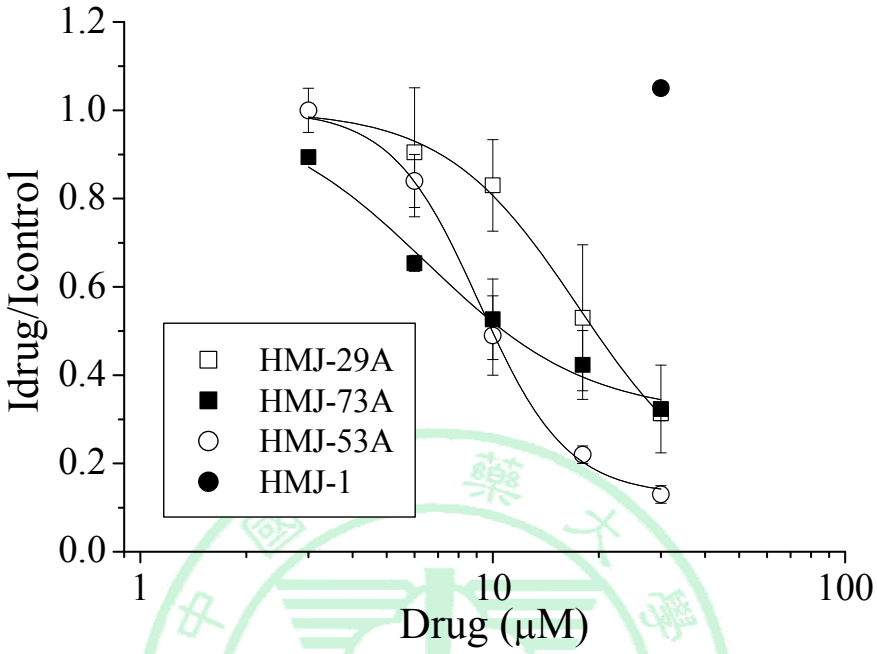

第六章：參考文獻

Andalib, P., Consiglio, J.F., Trapani, J.G., and Korn, S.J. (2004). The external TEA binding site and C-type inactivation in voltage-gated potassium channels. Biophys J *87*, 3148-3161.

Baukrowitz, T., and Yellen, G. (1996). Two functionally distinct subsites for the binding of internal blockers to the pore of voltage-activated K+ channels. Proc Natl Acad Sci U S A *93*, 13357-13361.

Bayliss, D.A., Talley, E.M., Sirois, J.E., and Lei, Q. (2001). TASK-1 is a highly modulated pH-sensitive 'leak' K(+) channel expressed in brainstem respiratory neurons. Respir Physiol *129*, 159-174.

Bowlby, M.R., Fadool, D.A., Holmes, T.C., and Levitan, I.B. (1997). Modulation of the Kv1.3 potassium channel by receptor tyrosine kinases. J Gen Physiol *110*, 601-610.

Berne, R.M., Levy, M.N., Koeppen B.M., and Stanton B.A., (1998). Physiology. St. Louis, Missouri press.

Choe, S. (2002). Potassium channel structures. Nat Rev Neurosci *3*, 115-121.

Choe, S., Kreusch, A., and Pfaffinger, P.J. (1999). Towards the three-dimensional structure of voltage-gated potassium channels. Trends Biochem Sci *24*, 345-349.

Choi, K.L., Aldrich, R.W., and Yellen, G. (1991). Tetraethylammonium blockade distinguishes two inactivation mechanisms in voltage-activated K+ channels. Proc Natl Acad Sci U S A *88*, 5092-5095.

Choi, K.L., Mossman, C., Aube, J., and Yellen, G. (1993). The internal quaternary ammonium receptor site of Shaker potassium channels. Neuron *10*, 533-541.

Claydon, T.W., Vaid, M., Rezazadeh, S., Kehl, S.J., and Fedida, D. (2007). 4-aminopyridine prevents the conformational changes associated with p/c-type inactivation in shaker channels. J Pharmacol Exp Ther *320*, 162-172.

Cogolludo, A., Moreno, L., Bosca, L., Tamargo, J., and Perez-Vizcaino, F. (2003). Thromboxane A2-induced inhibition of voltage-gated K+ channels and pulmonary vasoconstriction: role of protein kinase Czeta. Circ Res *93*, 656-663.

Cordero-Morales, J.F., Jogini, V., Lewis, A., Vasquez, V., Cortes, D.M., Roux, B., and Perozo, E. (2007). Molecular driving forces determining potassium channel slow inactivation. Nat Struct Mol Biol *14*, 1062-1069.

Doyle, D.A., Morais Cabral, J., Pfuetzner, R.A., Kuo, A., Gulbis, J.M., Cohen, S.L., Chait, B.T., and MacKinnon, R. (1998). The structure of the potassium channel: molecular basis of K+ conduction and selectivity. Science *280*, 69-77.

Fedida, D., Maruoka, N.D., and Lin, S. (1999). Modulation of slow inactivation in human cardiac Kv1.5 channels by extra- and intracellular permeant cations. J Physiol *515 (Pt 2)*, 315-329.

Goldstein, S.A., Price, L.A., Rosenthal, D.N., and Pausch, M.H. (1996). ORK1, a potassium-selective leak channel with two pore domains cloned from Drosophila melanogaster by expression in Saccharomyces cerevisiae. Proc Natl Acad Sci U S A *93*, 13256-13261.

Gulbis, J.M., Zhou, M., Mann, S., and MacKinnon, R. (2000). Structure of the cytoplasmic beta subunit-T1 assembly of voltage-dependent K+ channels. Science *289*, 123-127.

Holmgren, M., Jurman, M.E., and Yellen, G. (1996). N-type inactivation and the S4-S5 region of the Shaker K+ channel. J Gen Physiol *108*, 195-206.

Hoshi, T., Zagotta, W.N., and Aldrich, R.W. (1990). Biophysical and molecular mechanisms of Shaker potassium channel inactivation. Science *250*, 533-538.

Hille, B., (2001). Ion channels of excitable membranes. Sunderland, Mass.: Sinauer press.

Hour, M.J., Huang, L.J., Teng, C.M., Kuo, S.C., (2000). Synthesis and antiplatelet activity of alkoxy derivatives of 2-phenylquinazolines. Chin. Pharm. J. *52*, 167-177.

Jahangir, A., and Terzic, A. (2005). K(ATP) channel therapeutics at the bedside. J Mol Cell Cardiol *39*, 99-112.

Jiang, Y., Lee, A., Chen, J., Ruta, V., Cadene, M., Chait, B.T., and MacKinnon, R. (2003). X-ray structure of a voltage-dependent K+ channel. Nature *423*, 33-41.

Kindler, C.H., Yost, C.S., and Gray, A.T. (1999). Local anesthetic inhibition of baseline potassium channels with two pore domains in tandem. Anesthesiology *90*, 1092-1102.

Kiss, L., Immke, D., LoTurco, J., and Korn, S.J. (1998). The interaction of Na+ and K+ in voltage-gated potassium channels. Evidence for cation binding sites of different affinity. J Gen Physiol *111*, 195-206.

Klemic, K.G., Kirsch, G.E., and Jones, S.W. (2001). U-type inactivation of Kv3.1 and Shaker potassium channels. Biophys J *81*, 814-826.

Kukuljan, M., Labarca, P., and Latorre, R. (1995). Molecular determinants of ion conduction and inactivation in K+ channels. Am J Physiol *268*, C535-556.

Kurata, H.T., Doerksen, K.W., Eldstrom, J.R., Rezazadeh, S., and Fedida, D. (2005). Separation of P/C- and U-type inactivation pathways in Kv1.5 potassium channels. J Physiol *568*, 31-46.

Kurata, H.T., and Fedida, D. (2006). A structural interpretation of voltage-gated potassium channel inactivation. Prog Biophys Mol Biol *92*, 185-208.

Kurata, H.T., Soon, G.S., Eldstrom, J.R., Lu, G.W., Steele, D.F., and Fedida, D. (2002). Amino-terminal determinants of U-type inactivation of voltage-gated K+ channels. J Biol Chem *277*, 29045-29053.

Kurata, H.T., Soon, G.S., and Fedida, D. (2001). Altered state dependence of c-type inactivation in the long and short forms of human Kv1.5. J Gen Physiol *118*, 315-332.

Ledoux, J., Chartier, D., and Leblanc, N. (1999). Inhibitors of calmodulin-dependent protein kinase are nonspecific blockers of voltage-dependent K+ channels in vascular myocytes. J Pharmacol Exp Ther *290*, 1165-1174.

Leung, Y.M., Ahmed, I., Sheu, L., Gao, X., Hara, M., Tsushima, R.G., Diamant, N.E., and Gaisano, H.Y. (2006). Insulin regulates islet alpha-cell function by reducing KATP channel sensitivity to adenosine 5'-triphosphate inhibition. Endocrinology *147*, 2155-2162.

Leung, Y.M., Kang, Y., Gao, X., Xia, F., Xie, H., Sheu, L., Tsuk, S., Lotan, I., Tsushima, R.G., and Gaisano, H.Y. (2003). Syntaxin 1A binds to the cytoplasmic C terminus of Kv2.1 to regulate channel gating and trafficking. J Biol Chem *278*, 17532-17538.

Lopez-Barneo, J., Hoshi, T., Heinemann, S.H., and Aldrich, R.W. (1993). Effects of external cations and mutations in the pore region on C-type inactivation of Shaker potassium channels. Receptors Channels *1*, 61-71.

Loussouarn, G., Rose, T., and Nichols, C.G. (2002). Structural basis of inward rectifying potassium channel gating. Trends Cardiovasc Med *12*, 253-258.

MacKinnon, R., Aldrich, R.W., and Lee, A.W. (1993). Functional stoichiometry of Shaker potassium channel inactivation. Science *262*, 757-759.

McKay, M.C., and Worley, J.F., 3rd (2001). Linoleic acid both enhances activation and blocks Kv1.5 and Kv2.1 channels by two separate mechanisms. Am J Physiol Cell Physiol *281*, C1277-1284.

Molina, A., Castellano, A.G., and Lopez-Barneo, J. (1997). Pore mutations in Shaker K+ channels distinguish between the sites of tetraethylammonium blockade and C-type inactivation. J Physiol *499 (Pt 2)*, 361-367.

Nerbonne, J.M. (2000). Molecular basis of functional voltage-gated K+ channel diversity in the mammalian myocardium. J Physiol *525 Pt 2*, 285-298.

Oliver, D., Lien, C.C., Soom, M., Baukrowitz, T., Jonas, P., and Fakler, B. (2004). Functional conversion between A-type and delayed rectifier K+ channels by membrane lipids. Science *304*, 265-270.

Oxford, G.S., and Wagoner, P.K. (1989). The inactivating K+ current in GH3 pituitary cells and its modification by chemical reagents. J Physiol *410*, 587-612.

Poolos, N.P., and Johnston, D. (1999). Calcium-activated potassium conductances contribute to action potential repolarization at the soma but not the dendrites of hippocampal CA1 pyramidal neurons. J Neurosci *19*, 5205-5212.

Rezazadeh, S., Claydon, T.W., and Fedida, D. (2006). KN-93 (2-[N-(2-hydroxyethyl)]-N-(4-methoxybenzenesulfonyl)]amino-N-(4-chlorocinnamyl)-N-methylbenzylamine),a calcium/calmodulin-dependent protein kinase II inhibitor, is a direct extracellular blocker of voltage-gated potassium channels. J Pharmacol Exp Ther *317*, 292-299.

Sheng, M., Liao, Y.J., Jan, Y.N., and Jan, L.Y. (1993). Presynaptic A-current based on heteromultimeric K+ channels detected in vivo. Nature *365*, 72-75.

Sheng, M., Tsaur, M.L., Jan, Y.N., and Jan, L.Y. (1994). Contrasting subcellular localization of the Kv1.2 K+ channel subunit in different neurons of rat brain. J Neurosci *14*, 2408-2417.

Shimada, H., Uta, D., Nabekura, J., and Yoshimura, M. (2007). Involvement of Kv channel subtypes on GABA release in mechanically dissociated neurons from the rat substantia nigra. Brain Res *1141*, 74-83.

Sun, H.S., Feng, Z.P., Barber, P.A., Buchan, A.M., and French, R.J. (2007). Kir6.2-containing ATP-sensitive potassium channels protect cortical neurons from ischemic/anoxic injury in vitro and in vivo. Neuroscience *144*, 1509-1515.

Wang, S., Morales, M.J., Qu, Y.J., Bett, G.C., Strauss, H.C., and Rasmusson, R.L. (2003). Kv1.4 channel block by quinidine: evidence for a drug-induced allosteric effect. J Physiol *546*, 387-401.

Wang, Y.J., Lin, M.W., Lin, A.A., and Wu, S.N. (2008). Riluzole-induced block of voltage-gated Na+ current and activation of BKCa channels in cultured differentiated human skeletal muscle cells. Life Sci *82*, 11-20.

Yamada, K., and Inagaki, N. (2005). Neuroprotection by KATP channels. J Mol Cell Cardiol *38*, 945-949.

Yellen, G. (2002). The voltage-gated potassium channels and their relatives. Nature *419*, 35-42.

Zagotta, W.N., Hoshi, T., and Aldrich, R.W. (1990). Restoration of inactivation in mutants of Shaker potassium channels by a peptide derived from ShB. Science *250*, 568-571.

附 錄一：
SCI 期刊之
文章發表

Neuropharmacology 54 (2008) 1128–1135

Contents lists available at ScienceDirect

Neuropharmacology

journal homepage: www.elsevier.com/locate/neuropharm

HMJ-53A accelerates slow inactivation gating of voltage-gated K^+ channels in mouse neuroblastoma N2A cells

Chia-Chia Chao [a], Jeffrey Shieh [b], Sheng-Chu Kuo [c], Bor-Tsang Wu [d], Mann-Jen Hour [b,**], Yuk-Man Leung [a,e,*]

[a] Department of Physiology, China Medical University, Taichung 404, Taiwan, ROC
[b] School of Pharmacy, China Medical University, Taichung 404, Taiwan, ROC
[c] Graduate Institute of Pharmaceutical Chemistry, China Medical University, Taichung 404, Taiwan, ROC
[d] Department of Physical Therapy, China Medical University, Taichung 404, Taiwan, ROC
[e] Graduate Institute of Neural and Cognitive Sciences, China Medical University, Taichung 404, Taiwan, ROC

ARTICLE INFO

Article history:
Received 7 January 2008
Received in revised form 10 March 2008
Accepted 12 March 2008

Keywords:
HMJ-53A
Voltage-gated K^+ channels
C-type inactivation
Electrophysiology
Nerve cells

ABSTRACT

Voltage-gated K^+ (Kv) channels are important in repolarization of excitable cells such as neurons and endocrine cells. Kv channel gating exhibits slow inactivation (slow current decay) during continuous depolarization. The molecular mechanism involved in such slow inactivation is not completely understood, but evidence has suggested that it involves a restriction of the outer channel pore surrounding the selectivity filter. Pharmacological tools probing this slow inactivation process are scarce. In this work we reported that bath application of HMJ-53A (30 μM), a novel compound, could drastically speed up the slow decay (decay $\tau = 1677 \pm 120$ ms and 85.6 ± 7.7 ms, respectively, in the absence and presence of HMJ-53A) of Kv currents in neuroblastoma N2A cells. HMJ-53A also significantly left-shifted the steady-state inactivation curve by 12 mV. HMJ-53A, however, did not affect voltage-dependence of activation and the kinetics of channel activation. Intracellular application of this drug through patch pipette dialysis was ineffective at all in accelerating the slow current decay, suggesting that HMJ-53A acted extracellularly. Blockade of currents by HMJ-53A did not require an open state of channels. In addition, the inactivation time constants and percentage block of Kv currents in the presence of HMJ-53A were independent of the (i) degree of depolarization and (ii) intracellular K^+ concentration. Therefore, this drug did not appear to directly occlude the outer channel pore during stimulation (depolarization). Taken together, our results suggest that HMJ-53A selectively affected (accelerated) the slow inactivation gating process of Kv channels, and could thus be a selective and novel probe for the inactivation gate.

1. Introduction

In excitable cells such as neurons and endocrine cells, voltage-gated K^+ (Kv) channels are important in repolarization of the plasma membrane by allowing K^+ efflux (Hille, 2001). The Kv channel α-subunit (conducting pore) comprises of four polypeptides clustering around a central pore, each polypeptide subunit possessing six transmembrane helices (S1–S6) (Choe et al., 1999). S4 is the voltage sensor while between S5 and S6 is the P-loop; the P-loops from the four polypeptide subunits form the K^+ selectivity filter (Choe, 2002; Yellen, 2002). When Kv channels open in response to depolarization, the S6 helices, being (part of) the activation gate, swing open, allowing intracellular K^+ to gain access to the internal vestibule of the channel (Choe, 2002; Yellen, 2002). During the time course of depolarization, while the activation gate still opens, Kv channels immediately begin to inactivate.

There are two main types of inactivation, one fast and one slow. For the fast type of inactivation, the cytoplasmic N-terminus of certain Kv channels (Kv1.4, Kv3.1 and Kv4.2) forms a "ball-and-chain", plugging the opened Kv channel at the internal vestibule (Kukuljan et al., 1995). The rate is fast so that substantial inactivation can happen within a 100 ms or so. This fast inactivation has been termed N-type inactivation (Kukuljan et al., 1995). A slow type of inactivation can happen in almost all Kv channels (with or

* Corresponding author. Department of Physiology, China Medical University, Taichung 404, Taiwan, ROC. Tel.: +886 4 22053366x2185; fax: +886 4 22076853.
** Corresponding author. Tel.: +886 4 22053366x5123; fax: +886 4 24730249.
E-mail addresses: mjhou@mail.cmu.edu.tw (M.-J. Hour), ymleung@mail.cmu.edu.tw (Y.-M. Leung).

0028-3908/$ – see front matter © 2008 Elsevier Ltd. All rights reserved.
doi:10.1016/j.neuropharm.2008.03.006

without N-type inactivation). This is manifested as a slower decay of Kv currents during persistent depolarization, and depending on individual Kv members, the current decay spans from a fraction of a second to a few seconds (Kurata and Fedida, 2006). This slow inactivation has been termed C-type inactivation and happens in many Kv channels, exemplified by members such as Kv1.5 and Kv2.1 (Kurata et al., 2001; Andalib et al., 2004). The molecular mechanism involved in such slow inactivation is not completely understood, but evidence has suggested that it involves a collapse or constriction of the outer channel pore surrounding the selectivity filter (Hille, 2001; also see review by Kurata and Fedida, 2006). A residue at the external pore mouth, T449 of the *Shaker* channel (Kv1 family), has been identified to be involved in C-type inactivation. Mutation of this amino acid to arginine, lysine, alanine or glutamate accelerated, while mutation to valine or tyrosine, retarded C-type inactivation (López-Barneo et al., 1993). Recent evidence also supports a mechanistic model in which the interaction strength (via hydrogen bonds) between residues in the selectivity filter and the adjacent pore helix is crucial for C-type inactivation (Cordero-Morales et al., 2007). Thus, in Kv1.2, mutating Val370 into Glu370 renders possible a strong interaction with Asp379; such interaction acts as a molecular spring to collapse the selectivity filter (Cordero-Morales et al., 2007).

Kv channel inactivation affects action potential contours and spiking frequency and thus significantly modulates neuronal excitability (Hille, 2001). Drugs, which alter Kv channel inactivation gating, could therefore alter neuronal excitability. Chemicals such as 4-acetamido-4′-isothiocyano-2,2′-disulphonic stilbene (SITS) and *N*-bromoacetamide (NBA) have been demonstrated to strongly suppress N-type inactivation of Kv channels in GH_3 pituitary cells (Oxford and Wagoner, 1989). However, selective pharmacological tools probing the C-type inactivation process have been lacking. We previously showed that HMJ-53A, a newly synthesized compound, could inhibit arachidonic acid-induced platelet aggregation with an IC_{50} value of 1.60 μM (13 times more potent than aspirin) (Hour et al., 2000). We suspected that such anti-aggregation activity could be attributed to HMJ-53A-induced ion channel blockade. In this work we examined if HMJ-53A would modulate K^+ currents in mouse neuroblastoma N2A cells. We here provided convincing evidence to show that HMJ-53A acted extracellularly to drastically accelerate C-type inactivation of Kv channels without altering activation gating. HMJ-53A could thus be a potential probe for the inactivation gate.

2. Materials and methods

2.1. Chemicals and cell culture

HMJ-53A was synthesized according to our previously reported protocol (Hour et al., 2000):

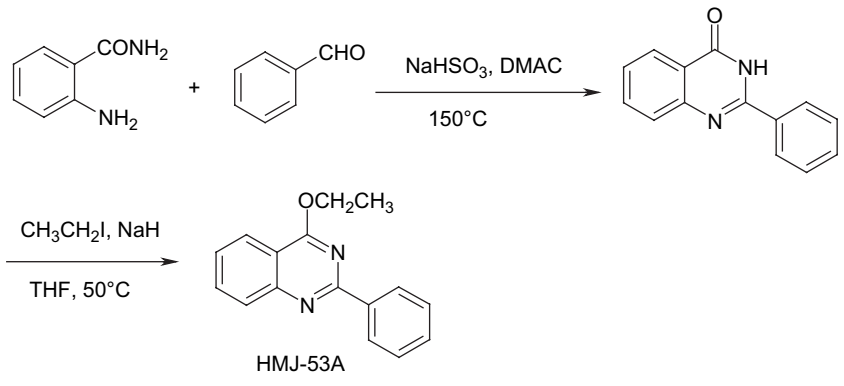

There was no cytotoxicity caused by 30 μM HMJ-53A in N2A cells, as judged by the trypan blue exclusion test (viability > 95%) and MTT assay (data not shown). TEA was purchased from Sigma (St. Louis, MO). N2A cells and PC12 cells were grown at 37 °C in 5% CO_2 in Dulbecco's modified Eagle's medium (DMEM) supplemented with 10% fetal bovine serum (Invitrogen, Carlsbad, CA) and penicillin–streptomycin (100 units/ml, 100 μg/ml) (Invitrogen).

2.2. Electrophysiology

Electrophysiological experiments were performed as previously reported (Leung et al., 2003). N2A cells were voltage-clamped in the whole-cell configuration. Thin-walled borosilicate glass tubes (OD 1.5 mm, ID 1.10 mm, Sutter Instrument, Novato, CA) were pulled with a micropipette puller (P-87, Sutter Instrument), and then heat polished by a microforge (Narishige Instruments, Inc., Sarasota, FL). The typical pipette resistance filled with intracellular solution, containing (mM): 140 KCl, 1 $MgCl_2$, 1 EGTA, 10 HEPES, and 5 MgATP (pH 7.25 adjusted with KOH), was 4–7 MΩ. The bath solution contained (mM): 140 NaCl, 4 KCl, 1 $MgCl_2$, 2 $CaCl_2$, 10 HEPES (pH 7.4 adjusted with NaOH). The currents were recorded using an EPC-10 amplifier with Pulse 8.60 acquisition software and analyzed by Pulsefit 8.60 software (HEKA Electronik, Lambrecht, Germany). Data were filtered at 2 kHz and sampled at 10 kHz. After a whole-cell configuration was established, the cells were held at −70 mV and subject to various protocols as detailed in Section 3 and the legends. All experiments were performed at room temperature (~22 °C).

Concentration-response curve for HMJ-53A inhibition of steady-state Kv currents is fit by the Hill equation:

$$I_{drug}/I_{control} = 1/\{1 + ([\text{HMJ-53A}]/K_d)^n\}$$

where I_{drug} is the steady-state current in the presence of HMJ-53A, $I_{control}$ is the steady-state current in the absence of HMJ-53A, [HMJ-53A] is the concentration of HMJ-53A in the bath, K_d is the apparent dissociation constant, and n is the Hill coefficient.

Curves showing voltage-dependence of activation in Kv channels are usually generated using tail current analysis. However, as the Kv currents in the presence of HMJ-53A inactivated very quickly, tail current analysis is not accurate enough. Therefore, Kv currents were stimulated with increasing depolarization, and conductance (G) was calculated as:

$$G = I/V - V_r$$

where $V_r = (RT/zF)\ln(\text{Ko}/\text{Ki})$.

V is the applied voltage, V_r is the reversal potential of K^+, I is the current, R is the universal gas constant, T is the temperature, z is the ion valency (+1 in this case) and F is the Faraday constant. Ko and Ki represent bath and pipette K^+ concentrations, respectively.

Data for voltage-dependence of activation and steady-state inactivation were fit by the Boltzmann equation: $G/G_{max} = 1/\{1 + \exp[(V_{1/2} - V)/k]\}$ (for fitting voltage-dependence of activation), or $I/I_{max} = 1/\{1 + \exp[(V - V_{1/2})/k]\}$ (for fitting steady-state inactivation), where $V_{1/2}$ is the half-maximal activation potential (for voltage-dependence of activation) or the half-maximal inactivation potential (for steady-state inactivation), and k the slope factor.

2.3. Statistical analysis

Data are presented as mean ± SEM. Unpaired or paired student's t test was used where appropriate to compare two groups, and a value of $p < 0.05$ was considered to have significant difference.

3. Results

3.1. HMJ-53A acted extracellularly to accelerate current decay

Depolarization of N2A cells triggered an outward current, which decayed very slowly (Fig. 1A, B). This slow decay has been attributed to C-type inactivation (Kurata and Fedida, 2006). The cells were continuously pulsed with depolarizing voltages and the current decay rate did not change significantly over time (Fig. 1A, B) (decay τ at time 0 and 10.7 min = 1440 ± 170 ms and 1376 ± 164 ms, respectively, $n = 5$). As shown in Fig. 1C, D, extracellular application of 30 μM HMJ-53A accelerated the decay, with stronger acceleration developing with time; and when the effect of HMJ-53A reached equilibrium, the decay time constant was drastically reduced to <0.1 s (decay $\tau = 85.6 \pm 7.7$ ms, $n = 16$; decay τ at time 0 = 1677 ± 120 ms, $n = 19$; $p < 0.05$). The effect of HMJ-53A was fully reversible, as the current decay rate gradually returned to pre-drug level after a 10–12 min washout (Fig. 1E, F; 95.3 ± 16.5% recovery, $n = 4$).

Fig. 2 shows the concentration-dependent effect of HMJ-53A on inhibiting the steady-state currents. An IC_{50} of 9.2 μM was obtained from the Hill plot and the Hill coefficient was remarkably high (3.5), suggesting multiple drug binding sites exhibiting positive cooperativity.

We also examined whether HMJ-53A affected Kv current decay rate in PC12 cells. With +30 mV stimulation, the Kv currents had a decay τ of 762 ± 272 ms; with 30 μM HMJ-53A treatment the decay τ at equilibrium became 77 ± 13 ms ($p < 0.05$, $n = 6$).

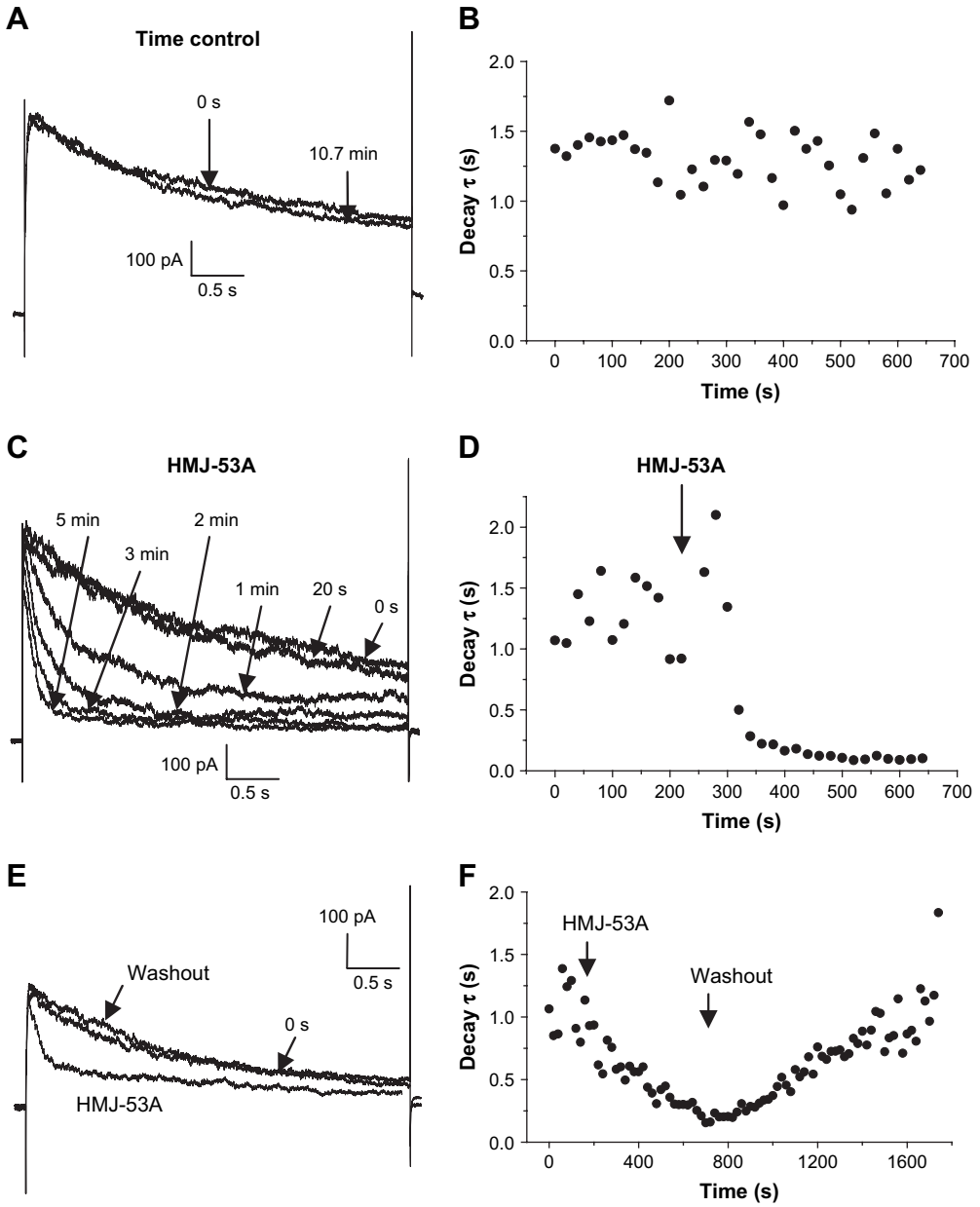

Fig. 1. HMJ-53A accelerated slow inactivation of Kv currents in N2A cells. (A) Representative traces showing outward K^+ currents triggered by +30 mV at time 0 and after 10.7 min in the absence of any treatment. (B) The decay time constants as observed in (A) are plotted against time. (C) Representative traces showing outward K^+ currents triggered by +30 mV before and after bath application of 30 μM HMJ-53A. (D) The decay time constants before and after HMJ-53A treatment as observed in (C) are plotted against time. (E) Representative traces showing outward K^+ currents triggered by +30 mV before and after 30 μM HMJ-53 addition, and after HMJ-53A washout. (F) The decay time constants as observed in (E) are plotted against time. Similar results were obtained in three more experiments.

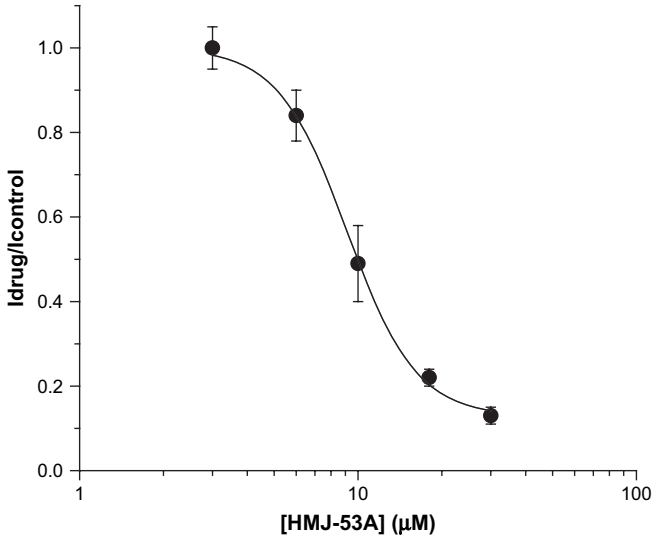

Fig. 2. Concentration-dependent inhibitory effects of HMJ-53A on Kv currents in N2A cells. With +30 mV stimulation, the steady-state Kv current in the presence of HMJ-53A is normalized with the maximum steady-state current (in the absence of drug) and then plotted against HMJ-53A concentration. The curve is fit with the Hill equation. Results are mean ± SEM from three to six cells.

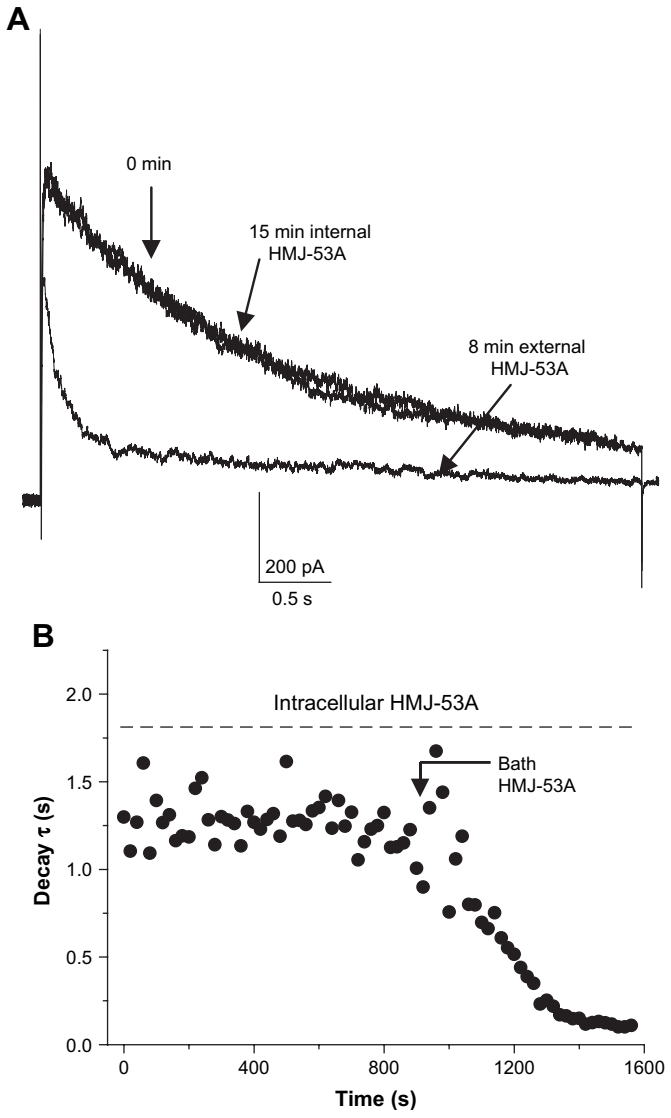

Fig. 3. Intracellularly applied HMJ-53A did not affect slow inactivation of Kv currents in N2A cells. (A) Representative traces showing outward K^+ currents triggered by +30 mV just after whole-cell configuration was established, after 15-min of 30 μM HMJ-53A dialysis and 8 min after bath application of 30 μM HMJ-53A to the same cell. (B) The decay time constants before and after HMJ-53A treatment as observed in (A) are plotted against time. Similar results were obtained in three more experiments.

Where did HMJ-53A act? In N2A cells, a 15-min intracellular dialysis of 30 μM HMJ-53A did not alter the decay rate (decay τ at time 0 and 15 min = 1270 ± 151 ms and 1418 ± 128 ms, respectively, $n = 4$), while a subsequent bath application of 30 μM HMJ-53A caused a substantial acceleration of current decay (decay τ at equilibrium = 58 ± 6 ms, $n = 3$) (Fig. 3A, B). These data suggest that HMJ-53A acted extracellularly.

3.2. HMJ-53A interacted with the closed state of the Kv channel

To resolve the question whether HMJ-53A interacted with the closed or open state of the Kv channel, N2A cell was first depolarized with a +30 mV pulse to record the currents (Fig. 4A). The cell was subsequently exposed to 30 μM HMJ-53A for 4 min without being stimulated with depolarizing pulses. Thereafter, the cell was stimulated again with a +30 mV pulse and the second current trace was recorded (Fig. 4B). The peak current magnitude was significantly reduced to 61.9 ± 5.3% of control after HMJ-53A exposure ($p < 0.05$, $n = 4$). Since no channel opening was triggered during the 4-min HMJ-53A treatment, the data suggest that HMJ-53A may block the closed state but not the opened state of Kv channels. Washout of HMJ-53A resulted in a 102.7 ± 3.8% recovery (Fig. 4C).

3.3. HMJ-53A did not appear to be a direct channel pore blocker

Did HMJ-53A act as a direct channel pore blocker? HMJ-53A might reside at the outer channel pore, and gain better access to a site at the outer vestibule (or selectivity filter) upon depolarization to account for the accelerated current decay. In other words, did HMJ-53A also have an affinity for a site at the pore of the opened channel? If the latter proposal is correct, HMJ-53A-channel interaction is expected to correlate positively with channel openness, manifested as faster current decay with increasing depolarization. We therefore examined whether different degrees of depolarization of N2A cells would affect the current decay rate in the presence of HMJ-53A (Fig. 5). In the absence of HMJ-53A, current decay rates at different depolarization pulses remained relatively constant, with extreme depolarization (>+70 mV) causing a deceleration of decay (Fig. 5A, C). In the presence of 30 μM HMJ-53A, current decay over a wide range of depolarization pulses (0 to +100 mV) was accelerated to almost the same extent (Fig. 5B, C). (It is noted that in N2A cells, Kv channel conductance increased steeply from −10 to 50 mV, Fig. 7B.) The results therefore argue against the notion that HMJ-53A occludes the outer pore and its affinity to the outer pore augments with depolarization.

As shown in Fig. 6A, the percentage block of steady-state Kv currents in N2A cells by 10 μM HMJ-53A (a concentration producing approximately a half-block, see Fig. 2) was independent of the applied voltages, further suggesting that drug-channel affinity did not appear to be correlated with the degree of channel opening. To further confirm that HMJ-53A did not block by directly occluding the channel pore, we examined the effect of intracellular K^+ concentration on HMJ-53A actions. If HMJ-53A directly occludes the pore, then HMJ-53A and K^+ could encounter each other in the pore itself. Thus, the lower the intracellular K^+ concentration the greater the block of K^+ efflux will be. Therefore, reducing the intracellular

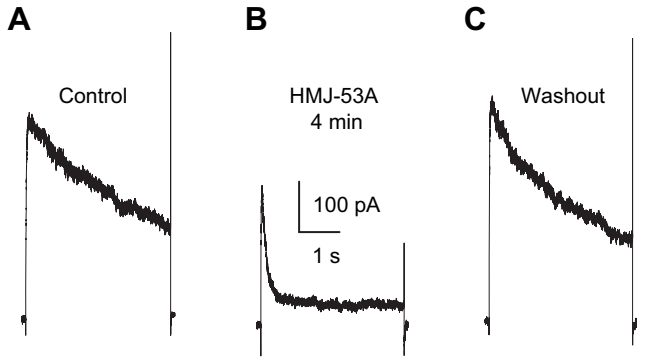

Fig. 4. HMJ-53A interacted with the closed state of the Kv channel in N2A cells. (A) The cell was firstly depolarized with a +30 mV pulse to record the currents. The cell was subsequently exposed to 30 μM HMJ-53A for 4 min without being stimulated with depolarization. (B) The cell was then stimulated again with a +30 mV pulse and the second current trace was recorded. (C) HMJ-53A was then washed out and the current was recorded with a +30 mV stimulation. Similar results were obtained in three more experiments.

K^+ concentration by half (i.e. to 70 mM) (with 140 mM sucrose added to keep intracellular solution iso-osmotic) is expected to enhance the effects of HMJ-53A. The latter maneuver indeed did not affect at all the percentage block or acceleration of C-type inactivation by 10 μM HMJ-53A in N2A cells (Fig. 6B, C), suggesting that HMJ-53A is unlikely a direct pore occluder.

3.4. HMJ-53A acted on the inactivation gate

The results above are incompatible with the view that HMJ-53A directly blocks at the outer pore mouth. Thus, it is likely that HMJ-53A accelerated the current decay by speeding up the closing of the inactivation gate, which is believed to be located at the selectivity filter itself. In other words, HMJ-53A may act by enhancing the rate of C-type inactivation. To probe into more details of how HMJ-53A may affect Kv channel inactivation in N2A cells, we examined if HMJ-53A affected steady-state inactivation of the Kv currents (Fig. 7A). In the presence of HMJ-53A, the steady-state inactivation curve left-shifted 12 mV ($V_{1/2} = -21.2 \pm 2.5$ mV and -33.0 ± 2.3 mV in the absence and presence of HMJ-53A, respectively; $p < 0.05$). However, HMJ-53A did not alter the slope factor (6.9 ± 1.3 and 5.9 ± 1.2 in the absence and presence of HMJ-53A, respectively; $p > 0.05$). Remarkably, in the control group, inactivation became progressively relieved with strong depolarization (>+50 mV), resulting in a U-type inactivation (Klemic et al., 2001; Kurata et al., 2002, 2005). The molecular mechanism for this mild refractoriness to inactivate at extreme depolarization is poorly understood. In the presence of HMJ-53A, the U-shape inactivation was not observed, suggesting that such refractoriness was overcome. These data further lend support to the notion that HMJ-53A enhanced the closing of the inactivation gate.

HMJ-53A speeded up the closing of the inactivation gate; did it affect the recovery of the inactivation gate? A dual-pulse protocol was employed to examine the recovery of the Kv currents in the absence and presence of HMJ-53A (Fig. 8). Quite unexpectedly, the currents in the absence and presence of HMJ-53A recovered at similar rates, with full recovery requiring a few seconds. The recovery is best fit to a double-exponential function. The fast recovery τ in the absence and presence of HMJ-53A was 187 ± 55 and 142 ± 38 ms, respectively ($p > 0.05$; $n = 6$–7). The slow recovery τ in the absence and presence of HMJ-53A was 3115 ± 982 and 1542 ± 810 ms, respectively ($p > 0.05$; $n = 6$–7). The data are intriguing as they suggest that HMJ-53A promoted the closing of the inactivation gate without retarding the latter's recovery.

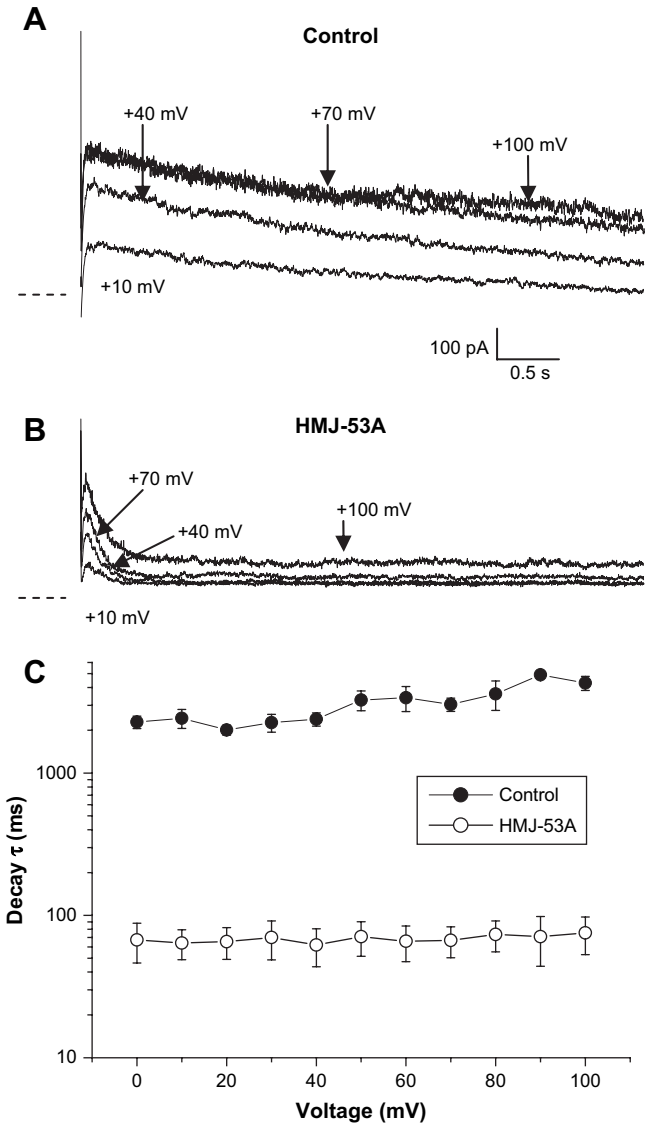

Fig. 5. Acceleration of current decay by HMJ-53A was voltage-independent. (A) Representative traces showing outward K^+ currents triggered by different depolarizing voltages in the absence of drug. (B) Representative traces showing outward K^+ currents triggered by different depolarizing voltages after about 15 min treatment with 30 μM HMJ-53A. (C) The decay time constants of currents obtained in the absence and presence of HMJ-53A were plotted against different voltages of depolarization. Results are mean ± SEM from four cells of each group.

3.5. Activation gating was not affected by HMJ-53A

We next investigated if HMJ-53A affected the activation gating of the Kv currents in N2A cells. The voltage-dependence of activation was not significantly affected by HMJ-53A (Fig. 7B) ($V_{1/2} = 12.8 \pm 3.2$ mV and 15.2 ± 1.6 mV in the absence and presence of HMJ-53A, respectively; $p > 0.05$). HMJ-53A also did not affect the slope factor (11.1 ± 0.5 and 13.9 ± 1.4 in the absence and presence of HMJ-53A, respectively; $p > 0.05$). Activation kinetics in control and HMJ-53A-treated cells were analyzed and shown to be comparable (Fig. 7C). Quantitative results in Fig. 7D show that currents activated at faster rates with increasing depolarization; HMJ-53A did not significantly alter the activation rates at various voltage pulses.

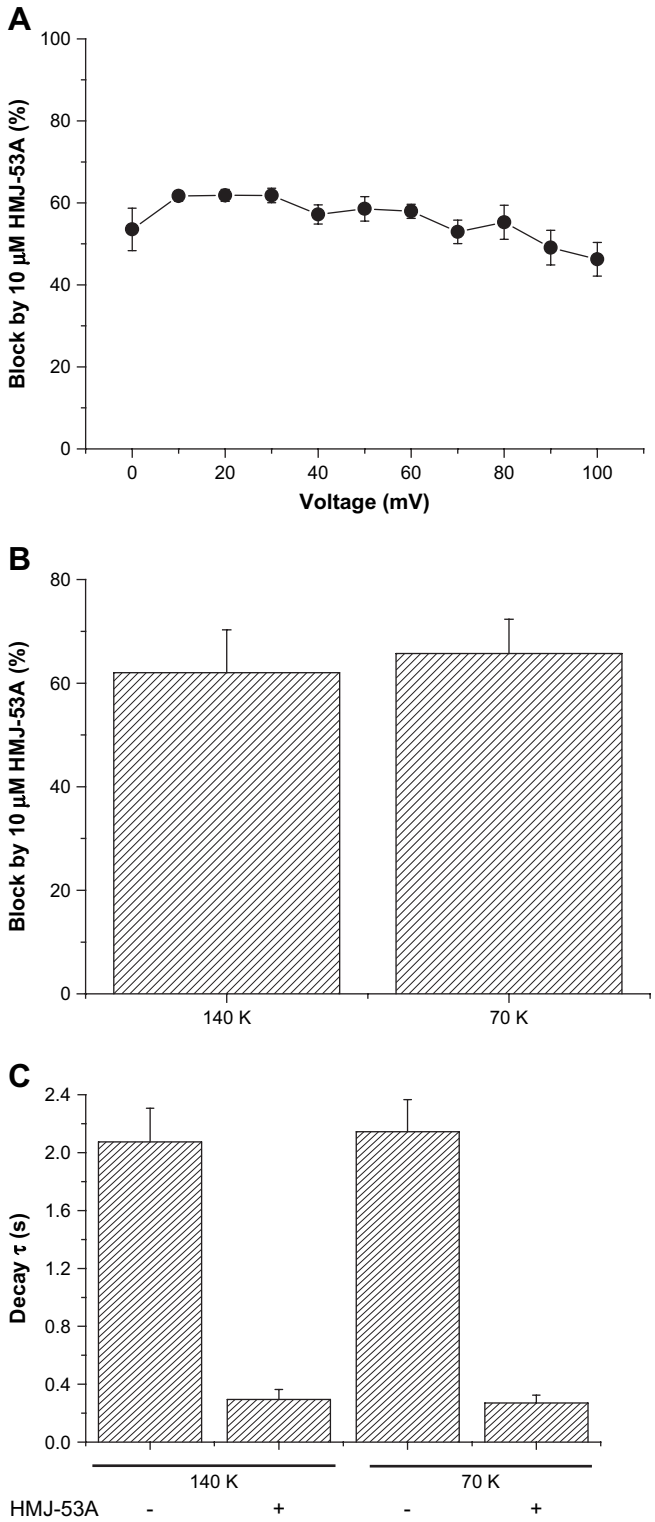

Fig. 6. HMJ-53A block was voltage-independent and not affected by intracellular K^+ concentration. (A) The percentage block of steady-state Kv currents by 10 μM HMJ-53A is plotted against the applied voltages. (B) The percentage block of steady-state Kv currents by 10 μM HMJ-53A in the presence of 70 or 140 mM intracellular (i.e. pipette) K^+. (C) The decay time constants of Kv currents (with and without 10 μM HMJ-53A) in the presence of 70 or 140 mM intracellular K^+. Results are mean ± SEM from four to five cells.

4. Discussion

The molecular mechanisms for C-type inactivation of Kv channels have not been fully understood, although it is believed that it involves squeezing or narrowing of the selectivity filter (or domains around it), hence restricting K^+ fluxes (Hille, 2001; Kurata and Fedida, 2006). Pharmacological probes for this C-type inactivation would prove useful in not only delineating the mechanism of C-type inactivation, but also the importance of C-type inactivation in modulating neuronal excitability with regard to action potential contours and firing frequency. However, specific probes for C-type inactivation are lacking.

In this work we reported that HMJ-53A accelerated the slow decay of Kv currents in N2A neuroblastoma cells. We provided evidence that HMJ-53A acted extracellulary, but not intracellularly, on the Kv channels in N2A cells (Fig. 3). The data in Fig. 4 may suggest two possibilities: HMJ-53A interacted with the closed state of the channel, or it interacted with the open state but the channel activation rate in the presence of HMJ-53A became slow enough to allow the block to prevent currents from reaching the peak. The latter possibility is unlikely as the activation kinetics was not affected by HMJ-53A (Fig. 7C, D). Another interpretation of the data in Fig. 4 is that as the channel just opened, HMJ-53A blocked directly at the outer pore so quickly as to overlap with current activation. We consider this possibility unlikely, as such proposal of a direct occlusion has to accommodate an initial very fast block, followed by a rate-limiting phase of block, which was manifested as the relatively slower decline in currents. If this second phase exists, it may represent another drug-channel affinity site available upon depolarization (or channel opening). Then, HMJ-53A-channel interaction is expected to correlate positively with degree of depolarization. However, the current decay rates at various depolarization voltages in the presence of HMJ-53A remain constant (Fig. 5), and percentage block was voltage-independent (Fig. 6A). These observations are inconsistent with the notion that HMJ-53A occludes the outer pore and that drug-pore interaction augments with depolarization. Further, we reasoned that if HMJ-53A directly occludes the pore, then HMJ-53A and K^+ would meet inside the pore itself; and it is expected that the lower the intracellular K^+ concentration the greater the block of K^+ efflux will be. However, the percentage block or acceleration of C-type inactivation by 10 μM HMJ-53A was not affected by drastically reducing the intracellular K^+ concentration (Fig. 6B, C).

Taken together, our data are therefore incompatible with HMJ-53A being a simple and direct channel pore occluder. It appears more likely that HMJ-53A acts on the inactivation gate. It could be envisaged that when the Kv channel is closed, HMJ-53A already inactivates the channel (thus, a blocker of closed state channel), and once the Kv channel opens, HMJ-53A speeds up inactivation gate closing.

In *Shaker* channels and several mammalian *Shaker* homologues, elevated extracellular K^+ concentration and extracellular TEA have been known to retard C-type inactivation (Choi et al., 1991; López-Barneo et al., 1993; Molina et al., 1997; Fedida et al., 1999). However, in N2A cells, Kv channel C-type inactivation rate was not significantly affected by TEA (3 mM) or raised extracellular K^+ (40 mM, by iso-osmotic substitution with Na^+) (data not shown). This could be due to the absence of mammalian *Shaker* homologues in N2A cells.

Intriguingly, HMJ-53A did not slow down the channel recovery rate (Fig. 8), indicating that there might be a very fast drug unbinding following repolarization. How can we reconcile this fast drug unbinding with the observation that HMJ-53A caused a tonic block of the Kv channels at their closed states? Based on the high Hill coefficient of HMJ-53A block (Fig. 2), there are multiple HMJ-53A binding sites. We propose that the HMJ-53A binding sites for tonic (closed channel) block may be separable from the site(s) for

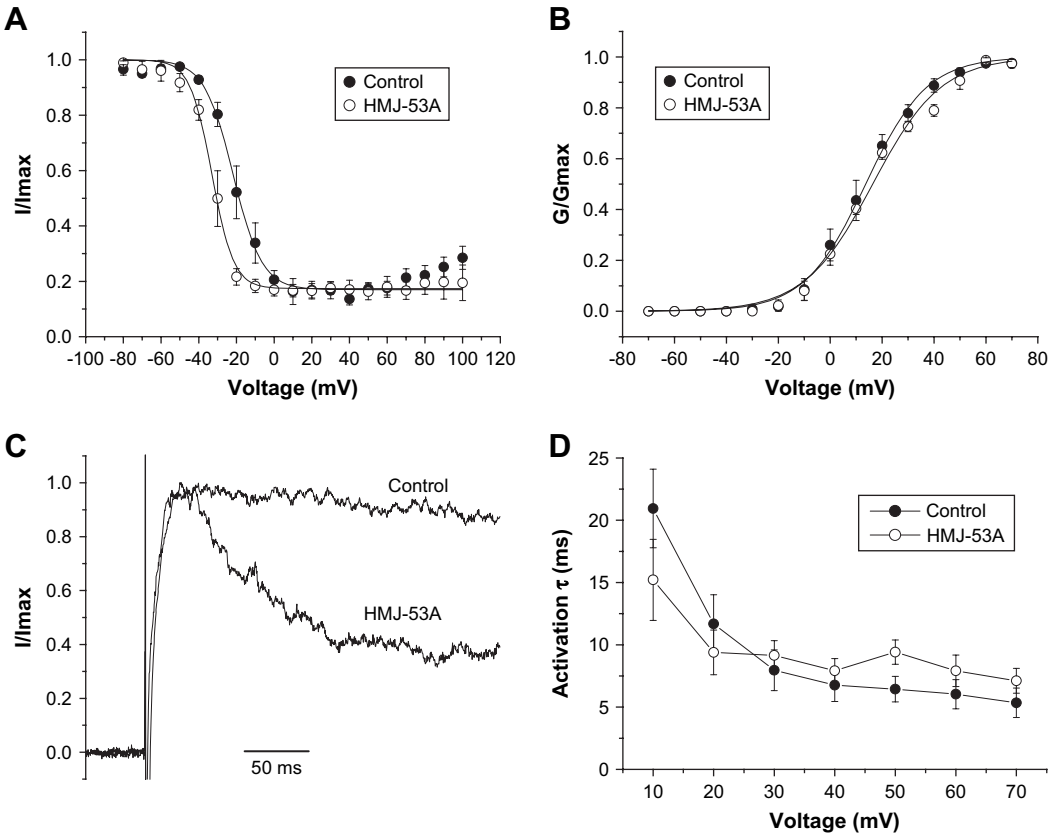

Fig. 7. HMJ-53A caused a left-shift in the steady-state inactivation curves without affecting activation gating. (A) Steady-state inactivation experiments were performed in cells treated with and without 30 μM HMJ-53A. In these experiments, a dual-pulse protocol was used in which a test pulse step of +70 mV was preceded by a long pre-pulse (10 s) of different potentials. The test pulse currents are normalized to the largest test pulse current and plotted against the pre-pulse voltages. Because the control group exhibited a "U-shape inactivation" phenomenon, the data from both groups are best fit by the Boltzmann equation from −80 mV to +50 mV only. Results are mean ± SEM from four cells of each group. (B) Voltage-dependence of activation: Kv currents were stimulated with increasing depolarization (from a holding potential of −70 mV and then 10 mV increments), and conductance (G) is calculated as described in Section 2. Conductances in the control group and HMJ-53A group are normalized with their respective maximum conductance (G_{max}) and then plotted against the applied depolarization voltages. The curves are fit with the Boltzmann equation. Results are mean ± SEM from four to six cells of each group. (C) Early phase of current traces showing activation kinetics is comparable in control and HMJ-53A-treated cells. The currents of the control and HMJ-53A-treated cells are normalized to their respective peak magnitude and overlapped for comparison. (D) Activation time constants were obtained by an exponential fit to the rising phase of the currents, and then plotted against the applied depolarization voltages. Results are mean ± SEM from six to eight cells of each group.

HMJ-53A interaction during slow inactivation. HMJ-53A may unbind from the latter site(s) fast enough during repolarization so that it does not retard channel recovery.

HMJ-53A-inactivation gate interaction also resulted in enhancement of steady-state inactivation of Kv channels at slight depolarization (Fig. 7A; −50 to −30 mV, voltages below activation threshold [see Fig. 7B]). Thus, HMJ-53A caused a 12 mV left-shift in the steady-state inactivation curve. Remarkably, the Kv currents in N2A cells exhibit a U-type inactivation. Thus, the inactivation gate became progressively reluctant to close with strong depolarization (>+50 mV). Kv1.5, Kv2.1 and Kv3.1 exhibit U-type inactivation (Klemic et al., 2001; Kurata et al., 2002, 2005); one or some of these channels may be present in N2A cells. The molecular mechanism for such mild refractoriness to inactivate at extreme depolarization is unknown. With HMJ-53A, such refractoriness was overcome (Fig. 7A), providing further support that HMJ-53A enhanced the closing of the inactivation gate. Does HMJ-53A affect the cytoplasmic activation gate? Here we have provided evidence to show that HMJ-53A did not significantly affect the voltage-dependence and kinetics of Kv channel activation (Fig. 7B–D). Taken together, the pharmacological profile suggests that HMJ-53A is a novel and specific probe for the Kv channel inactivation gate.

There have been a number of gating modifiers reported to enhance the inactivation gate. KN-93, acting in an extracellular manner, has been known to enhance slow inactivation of a number

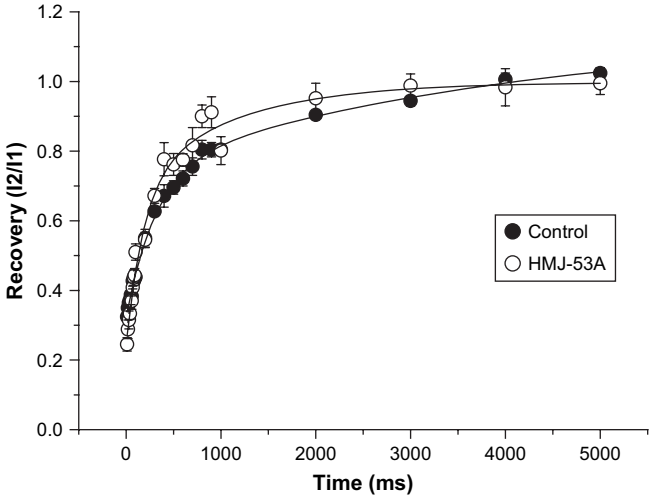

Fig. 8. Lack of effect of HMJ-53A on Kv current recovery. Current recovery experiments were performed in N2A cells treated with and without 30 μM HMJ-53A. In these experiments, a dual-pulse protocol was used in which the first test pulse (+30 mV, 5000 ms) and second test pulse (+30 mV, 200 ms) were separated by different time intervals. The maximum current amplitude of the second pulse (I_2) is normalized with the maximum current amplitude of the first pulse (I_1). The normalized data are plotted against the time intervals. The curves are fit with a double-exponential function. Results are mean ± SEM from four cells of each group.

of Kv channels (Ledoux et al., 1999; Rezazadeh et al., 2006). However, the drug effect of KN-93 is only partially reversible and KN-93 also affects the voltage-dependence of activation: slight left-shift and significant decrease, respectively, in activation curve and its Boltzmann slope factor (Rezazadeh et al., 2006). Linoleic acid has also been shown to accelerate slow inactivation of Kv1.5 and Kv2.1 by acting extracellularly but not intracellularly (McKay and Worley, 2001). However, linoleic acid also affects activation gating by causing a left-shift in the activation curve and acceleration of activation kinetics (McKay and Worley, 2001). Therefore, HMJ-53A, effects being fully reversible and selective for inactivation gating, would be much more desirable for probing the inactivation gate.

Quinidine has been shown to cause an acceleration of C-type inactivation (Wang et al., 2003). However, quinidine achieves this by an allosteric action as a consequence of intracellular open-channel block. Further, 4-aminopyridine, a Kv channel blocker acting intracellularly, has also been demonstrated to modulate (inhibit) C-type inactivation of *Shaker* channels (Claydon et al., 2007). These data raise the possibility that conformational changes at the cytoplasmic side of the channel could be a factor modulating C-type inactivation. In line with this thinking, it would be of interest to ask whether HMJ-53A affected the inactivation gate indirectly, by firstly causing channel conformational changes at the cytoplasmic side (via, for example, phosphorylation or changing intracellular pH). This appears unlikely for dual reasons. First, HMJ-53A did not show any effect when applied intracellularly. Second, staurosporine (100 nM, a wide-spectrum protein kinase inhibitor) and changes of pipette (therefore, intracellular) pH to extremes (pH 6.6 and 7.8) did not on their own alter rate of current decay or modulate HMJ-53A effect on C-type inactivation (data not shown). These negative results suggest it is unlikely that HMJ-53A acted on the plasma membrane, and then via certain signaling pathways, altered the intracellular conformation of Kv channels leading finally to modulation of C-type inactivation. Failure of intracellularly applied HMJ-53A to affect Kv currents also implies that HMJ-53A does not exert its effect via modulation of cytosolic factors or perturbation of membrane lipid homeostasis (Oliver et al., 2004).

Acknowledgments

Y.M.L. would like to thank China Medical University, Taiwan, and the Taiwan National Science Council for providing start-up funds (CMU95-049; CMU95-182; CMU96-125; NSC 95-2321-B-039-001-). M.J.H. would like to thank China Medical University, Taiwan for a research funding (CMU95-112).

References

Andalib, P., Consiglio, J.F., Trapani, J.G., Korn, S.J., 2004. The external TEA binding site and C-type inactivation in voltage-gated potassium channels. Biophys. J. 87, 3148–3161.

Choe, S., 2002. Potassium channel structures. Nat. Rev. Neurosci. 3, 115–121.

Choe, S., Kreusch, A., Pfaffinger, P.J., 1999. Towards the three-dimensional structure of voltage-gated potassium channels. Trends Biochem. Sci. 24, 345–349.

Choi, K.L., Aldrich, R.W., Yellen, G., 1991. Tetraethylammonium blockade distinguishes two inactivation mechanisms in voltage-activated K^+ channels. Proc. Natl. Acad. Sci. U.S.A. 88, 5092–5095.

Claydon, T.W., Vaid, M., Rezazadeh, S., Kehl, S.J., Fedida, D., 2007. 4-aminopyridine prevents the conformational changes associated with p/c-type inactivation in *Shaker* channels. J. Pharmacol. Exp. Ther. 320, 162–172.

Cordero-Morales, J.F., Jogini, V., Lewis, A., Vásquez, V., Cortes, D.M., Roux, B., Perozo, E., 2007. Molecular driving forces determining potassium channel slow inactivation. Nat. Struct. Mol. Biol. 14 (11), 1062–1069.

Fedida, D., Maruoka, N.D., Lin, S., 1999. Modulation of slow inactivation in human cardiac Kv1.5 channels by extra- and intracellular permeant cations. J. Physiol. 515, 315–329.

Hille, B., 2001. Ion Channels of Excitable Membranes. Sinauer press, Sunderland, Mass.

Hour, M.J., Huang, L.J., Teng, C.M., Kuo, S.C., 2000. Synthesis and antiplatelet activity of alkoxy derivatives of 2-phenylquinazolines. Chin. Pharm. J. 52, 167–177.

Klemic, K.G., Kirsch, G.E., Jones, S.W., 2001. U-type inactivation of Kv3.1 and *Shaker* potassium channels. Biophys. J. 81, 814–826.

Kukuljan, M., Labarca, P., Latorre, R., 1995. Molecular determinants of ion conduction and inactivation in K^+ channels. Am. J. Physiol. 268, 535–556.

Kurata, H.T., Doerksen, K.W., Eldstrom, J.R., Rezazadeh, S., Fedida, D., 2005. Separation of P/C- and U-type inactivation pathways in Kv1.5 potassium channels. J. Physiol. 568, 31–46.

Kurata, H.T., Fedida, D., 2006. A structural interpretation of voltage-gated potassium channel inactivation. Prog. Biophys. Mol. Biol. 92, 185–208.

Kurata, H.T., Soon, G.S., Eldstrom, J.R., Lu, G.W., Steele, D.F., Fedida, D., 2002. Amino-terminal determinants of U-type inactivation of voltage-gated K^+ channels. J. Biol. Chem. 277, 29045–29053.

Kurata, H.T., Soon, G.S., Fedida, D., 2001. Altered state dependence of c-type inactivation in the long and short forms of human Kv1.5. J. Gen. Physiol. 118, 315–332.

Leung, Y.M., Kang, Y., Gao, X., Xia, F., Xie, H., Sheu, L., Tsuk, S., Lotan, I., Tsushima, R.G., Gaisano, H.Y., 2003. Syntaxin 1A binds to the cytoplasmic C terminus of Kv2.1 to regulate channel gating and trafficking. J. Biol. Chem. 278, 17532–17538.

Ledoux, J., Chartier, D., Leblanc, N., 1999. Inhibitors of calmodulin-dependent protein kinase are nonspecific blockers of voltage-dependent K^+ channels in vascular myocytes. J. Pharmacol. Exp. Ther. 290, 1165–1174.

López-Barneo, J., Hoshi, T., Heinemann, S.H., Aldrich, R.W., 1993. Effects of external cations and mutations in the pore region on C-type inactivation of *Shaker* potassium channels. Recept. Channels 1, 61–71.

McKay, M.C., Worley III, J.F., 2001. Linoleic acid both enhances activation and blocks Kv1.5 and Kv2.1 channels by two separate mechanisms. Am. J. Physiol. Cell Physiol. 281, 1277–1284.

Molina, A., Castellano, A.G., Lopez-Barneo, J., 1997. Pore mutations in *Shaker* K^+ channels distinguish between the sites of tetraethylammonium blockade and C-type inactivation. J. Physiol. 499, 361–367.

Oliver, D., Lien, C.C., Soom, M., Baukrowitz, T., Jonas, P., Fakler, B., 2004. Functional conversion between A-type and delayed rectifier K^+ channels by membrane lipids. Science 304, 265–270.

Oxford, G.S., Wagoner, P.K., 1989. The inactivating K^+ current in GH3 pituitary cells and its modification by chemical reagents. J. Physiol. 410, 587–612.

Rezazadeh, S., Claydon, T.W., Fedida, D., 2006. KN-93 (2-[*N*-(2-hydroxyethyl)]-*N*-(4 methoxybenzenesulfonyl)]-amino-*N*-(4-chlorocinnamyl)-*N*-methylbenzylamine), a calcium/calmodulin-dependent protein kinase II inhibitor, is a direct extracellular blocker of voltage-gated potassium channels. J. Pharmacol. Exp. Ther. 317, 292–299.

Wang, S., Morales, M.J., Qu, Y.J., Bett, G.C., Strauss, H.C., Rasmusson, R.L., 2003. Kv1.4 channel block by quinidine: evidence for a drug-induced allosteric effect. J. Physiol. 546, 387–401.

Yellen, G., 2002. The voltage-gated potassium channels and their relatives. Nature 419, 35–42.

附錄二：獎狀

獎　　狀

第一名

趙家佳 君 參與由中國醫藥大學基礎醫學研究所於 97 年 5 月 2 日所舉辦之 2008 研究生成果發表會，發表口頭論文，表現優異

特頒此狀，以資鼓勵

中國醫藥大學

基礎醫學研究所

所長 黃志揚

中 華 民 國 九 十 七 年 五 月 二 日